Renewable and Sustainable Energy Reviews 151 (2021) 111531

Contents lists available at ScienceDirect

Renewable and Sustainable Energy Reviews

journal homepage: www.elsevier.com/locate/rser

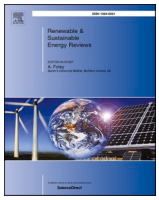

# Critical review and future prospects for desiccant coated heat exchangers: Materials, design, and manufacturing

Tomas Venegas [a], Ming Qu [a], Kashif Nawaz [b,*], Lingshi Wang [b]

[a] Lyles School of Civil Engineering, Purdue University, West Lafayette, IN, 47906, United States
[b] Oak Ridge National Laboratory, Oak Ridge, TN, 37831, United States

ARTICLE INFO

*Keywords:*
Solid desiccant
Adsorption
Dehumidification
Desiccant coated heat exchangers
Materials
Manufacturing

ABSTRACT

Solid desiccant dehumidification is a promising alternative to vapor compression-based air-dehumidification to reduce energy consumption and improve air quality. Desiccant coated heat exchanger (DCHE), as one type of solid desiccant dehumidification system, can improve system performance and efficiency. The thermal performance and moisture removal capability of the DCHE greatly influence its dehumidification performance.

The present work aims to critically analyze the designs, materials, and manufacturing methods of heat exchangers used for solid desiccant coating and look into recent developments in regular heat exchangers, potentially deployed as a substrate for DCHE applications. A comprehensive literature review of publications regarding solid desiccant materials, heat exchangers, manufacturing and coating methods, binder materials, and the performance of heat exchangers has been developed. Alternative heat exchangers are described as better options than fin and tube heat exchangers that have been considered thus far for DCHE applications. Additionally, the heat exchanger's manufacturing process and materials over their thermal and mass exchange performance have been analyzed. Despite the widespread use of fin and tube heat exchangers for solid desiccant coating, recent developments in heat exchanger design, and related fields such as manufacturing methods and materials, open the possibilities for their application in solid desiccant dehumidification systems.

Finally, the authors provide their outlook on possible developments of DCHE technology, aiming to increase systems' energy and dehumidification performance.

## 1. Introduction

Air humidity affects human thermal comfort and health [1]. Vapor compression systems (VCSs) are commonly used to control temperature and provide dehumidification capabilities, also called sensible and latent cooling, respectively. For latent cooling, VCS relies on the undercooling of process air below its dew point, which leads to the removal of excessive moisture by condensation. This process requires cooling the air below comfortable supply temperatures. Therefore a reheating process must follow the overcooling process before supplying air to the building, as the process of 1-4-5-2 is shown in Fig. 1. This process, therefore, is energy-inefficient. To overcome the weakness of the VCS, researchers have sought alternative dehumidification processes with better energy efficiency. One promising alternative is the solid-desiccant-based dehumidification (SDD) system. The SDD system uses solid desiccant materials coated on a substrate heat exchanger to remove the moisture from the air and supply the dehumidified air into the occupied space [2]. In solid desiccant-based dehumidification processes, capillary condensation happens due to increased water vapor concentration inside the pores of the desiccant material. The adsorption process gives off heat, which heats the desiccant material (the process from states 3 to 2 shown in Fig. 1), and the adsorption capability of the system drops. It is necessary to dry the solid desiccant material for sustaining the operation. The addition of heat is the most common process method to remove the adsorbed moisture in the saturated solid desiccant material. The adiabatic SDD needs simple cooling (the process from state 3 to 2, as shown in Fig. 1) to remove both the sensible heat of process air and the adsorption heat. Desiccant Coated Heat Exchanger (DCHE) system, a type of SDD system, uses internally cooled heat exchangers coated with solid desiccant material to remove the adsorption heat dehumidifying (the process from state 1 to 2 shown in Fig. 1). The cold water circulating inside the DCHE cools the DCHE and air to achieve higher adsorption capacity and partly sensible cooling. Therefore, the DCHE system can effectively meet sensible and latent loads without encountering performance degradation issues due to excessive cooling

* Corresponding author.
*E-mail address:* nawazk@ornl.gov (K. Nawaz).

https://doi.org/10.1016/j.rser.2021.111531
Received 18 July 2020; Received in revised form 10 July 2021; Accepted 24 July 2021
Available online 6 August 2021

**Nomenclature**

| *Term* | |
|---|---|
| AlPO | Aluminophosphates molecular sieves |
| AM | Addictive manufacturing |
| CS | Chitosan |
| DCHE | Desiccant coated heat exchanger |
| DW | Desiccant Wheel |
| EDM | Electric discharge machining |
| FFF | Fused filament fabrication |
| GSR | Gas side resistance |
| GSSR | Gas and solid side resistance |
| HEC | Hydroxyethyl cellulose |
| IER | Ion exchange resin |
| LiBr | Lithium bromide |
| LiCl | Lithium chloride |
| MC | Mesoporous Carbon |
| MIER | Modified ion exchange resin |
| MOF | Metal organic frameworks |
| MRC | Moisture removal capacity |
| PPI | Pores per inch |
| PVA | Polyvinyl alcohol |
| PTFE | Polytetrafluorethylene |
| SDD | Solid desiccant dehumidification |
| SLM | Selective laser melting |
| VCS | Vapor compression system |
| $\dot{m}_a$ | Air mass flow rate, kg/s |
| $\omega_{in}$ | Inlet air humidity, kg water/kg dry air |
| $\omega_{out}$ | Outlet air humidity, kg water/kg dry air |

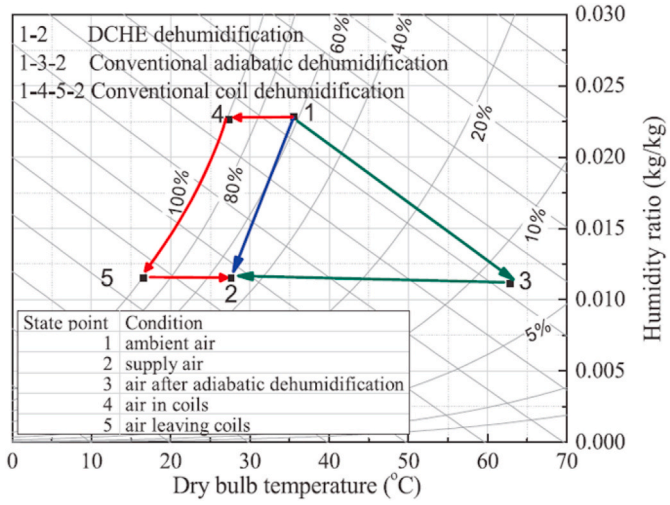


**Fig. 1.** Operation of conventional, adiabatic, and DCHE dehumidification systems [3].

and heating as observed in conventional vapor compression systems.

In the DCHE, the desiccants with high adsorption potential at relatively low temperatures can sustain the adsorption process for a longer time due to larger capacity, resulting in better performance than fixed bed SDD devices and desiccant wheels (DW). Moreover, internal cooling allows the air temperature to be maintained at desired conditions, reducing the need for sensible cooling devices deployed as an auxiliary process. It enables a unique control capability, which cannot be achieved by a conventional vapor compression-based system and the rotating enthalpy wheels. During the regeneration process in DCHE units, the cold fluid is replaced by a hot liquid, which increases air temperature, removing the moisture from the desiccant material to the airstream to accomplish the desiccant regeneration process.

Despite remarkable benefits, DCHE can be considered in the development stage, and there is a critical need to overcome some challenges before the technology can be implemented on a large scale. For instance, two DCHE units must be used in parallel to provide continuous dehumidification, which adds to the infrastructure. Regardless, this brings resiliency to the overall process, and if deployed appropriately, both systems can be operational where one is operating in dehumidification mode while the other is working in regeneration mode.

Fig. 2 shows the number of publications of the search results available on Scopus in June 2020 related to desiccant coated heat exchangers since 2010. The papers have been classified into the categories of

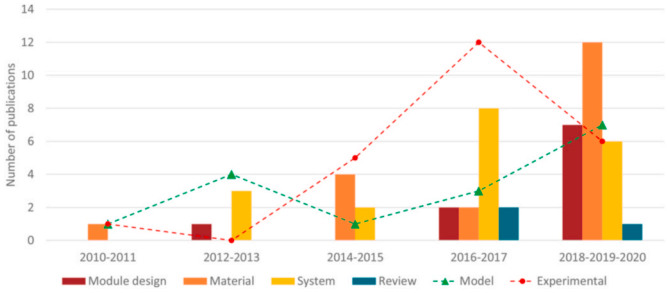


**Fig. 2.** Publications on solid desiccant exchanger collected in Scopus.

module design, materials, systems, and reviews. Additionally, a secondary classification between experimental and modeling works is provided. There is an increase in the number of publications from the period 2016–2017. The increase represents an increasing interest in the development of DCHE for dehumidification applications.

There are particular review articles on the subject. However, these have been focused on specific areas such as solid desiccant materials characterization, numerical models, and general reviews of the current state of the art [4–6]. The present study can be considered comprehensive since it covers a broad range of relevant aspects such as adsorbents, deployment strategies, substrate heat exchangers, and system integration. Apart from comprehensiveness, the current treatment of the subject is based on achieving a sustainable operation when such technology is implemented and relates to the practical implementation of the technology in the application, which is its two major distinguishing features. The authors have attempted to provide a thorough review of solid desiccant material about DCHE technology.

As a measure to compare the performance of different materials, the water adsorption isotherms for various materials have been studied and compared [4]. The desiccant materials reviewed include composite materials, nanoporous inorganic materials, and polymeric materials. The authors indicate that none of the reported materials possessed all the characteristics required, so further research in this area was needed. The mathematical models for the simulation of desiccant wheels have also been reviewed [5]. The models were classified into two main categories based on the explicit modeling of the solid side resistance to mass transfer, so the two categories are Gas Side Resistance Models (GSR) and Gas and Solid Side Resistance Models (GSSR). GSR refers to models in which the process of heat transfer is represented only by convection mass transfer. Meanwhile, in GSSR models, the water particle diffusion inside the solid desiccant material is also modeled. The review covers the main assumptions, partial differential equations,

auxiliary equations, boundary conditions, initial conditions, and numerical schemes implanted in each case to solve the models.

Besides the specific reviews for materials and mathematical models, general reviews of DCHE have been written [6]. The scope of the review covers solid desiccant materials, desiccant coating methods, binder materials, modeling, and system configurations. Different performance parameters have been included, such as Moisture Removal Capacity and thermal COP, which are useful to compare different system configurations, desiccant materials, and DCHE operational conditions. Finally, possible system configurations of DCHE based systems are presented. The final remarks of the author concur with other reviews (4), indicating that a significant advance in desiccant materials is required to improve the performance of DCHE.

As noted above, the fin and tube heat exchangers have been a preference for the solid desiccant coating to develop the device. However, limiting the design of the heat exchanger to traditional configurations has led to a major obstacle for the full exploitation and realization of the major benefits of the technology.

This paper aims to cover the gap in the literature about heat exchanger designs for DCHE applications. The paper investigates recent advances in DCHE heat exchangers and non-desiccant coated heat exchangers designs that could be applied to DCHE for the improvement of energy and dehumidification performance. The heat exchangers configurations are compared at aspects of the heat transfer performance, pressure drop, and air surface area to find suitable designs that could be used for solid desiccant applications. The comparison allows us to identify heat exchangers designs applied to DCHE for improving their dehumidification performance.

The materials used for currently studied DCHE are metals such as aluminum and copper, common materials for fin and tube heat exchangers. However, some novel heat exchanger configurations can be considered for use as DCHE, so a section of the review also deals with the different materials used in heat exchangers' design and physical properties. Furthermore, recent developments in solid desiccant and binder materials are also reviewed.

Some of the reviewed designs rely significantly on manufacturing methods different from the currently used parts-assembly process for fin and tube heat exchangers. The review also includes the manufacturing processes required for the heat exchangers. Finally, future research directions in the heat exchangers for DCHE have been recommended.

## 2. Solid desiccant dehumidification

### 2.1. Working principle

Adsorption is the process of enrichment of gas molecules on a surface of an interface. The enrichment can happen due to attraction forces and interactions such as polarization. The former case is called physisorption, and the latter chemisorption [7]. In the case of water adsorption by porous solid materials, the adsorption method is physisorption. Therefore adsorption principle will be further detailed next. Chemisorption will not be covered for being outside the scope of the operation of DCHE devices.

During the adsorption process, the area surrounding the adsorbent surface presents a lower water partial pressure than the humid air, and this differential drives the adsorption process [8]. The solid desiccant materials are highly porous materials with a range of pore sizes. The size of the pores has an impact on the adsorption process. For micropores (<2 [nm]), all adsorption takes place on its exposed surface. In comparison, for both mesopores (2 [nm] ~50 [nm]) and macropores (>50 [nm]), layers of adsorbed water molecules are stacked over each other. Therefore, there is an increase in partial water pressure in the deeper areas of the pores so that condensation occurs at temperatures lower than the bulk fluid dew point [7].

The adsorption process is exothermic, releasing heat to the process air and the solid desiccant [9]. As the temperature increases, the air capacity to contain water molecules increase, and the driving water vapor concentration differential between process air and solid desiccant diminishes, slowing the adsorption process. As the adsorption process continues, the solid desiccant surface saturates with water molecules and can no longer keep the adsorption process. At this point, the water molecules must be released from the solid desiccant, which is called desorption or regeneration. For regeneration, the solid desiccant material must be exposed to a heat source and dry air to lead to the moisture released from the solid desiccant [8]. The heat source increases the air's moisture retention capacity. Thus its relative humidity diminishes, creating a differential with the equivalent relative humidity on the solid desiccant material, which drives the moisture transfer from the desiccant to the regeneration air, a different air stream from the process air. Once the moisture has been removed from the solid desiccant layer, the DCHE can perform dehumidification again. A DCHE device operates in an adsorption-desorption cycle repeated continually. Therefore, typically two identical DCHE devices are needed to maintain the continuous provision of dehumidified air.

### 2.2. Dehumidification device

Solid desiccant-based dehumidification devices can be classified into fixed-bed dehumidifiers (Fig. 3a), desiccant wheels (Fig. 3b), and desiccant coated heat exchangers (Fig. 3c). Fixed-bed dehumidifiers are based on static layers of desiccant materials exposed to humid air. They require less maintenance than other alternatives or rotational operation dehumidification devices [10]. The desiccant material can be deployed as flat layers parallel to the flow direction [11] (case illustrated in Fig. 3a), hollow cylinders typical to flow direction layers [10], or packed beds [12]. Despite their more straightforward construction, they have been the subject of less experimental studies than desiccant wheels [13]. They do not require the use of binder materials mixed with the solid desiccant, which is an advantage compared to DW and DCHE [13]. A fixed-bed system needs at least two devices, which work in parallel to provide continuous dehumidification. Fixed bed dehumidifiers offer less control over the dehumidification process. Therefore, their outlet conditions depend entirely on the outdoor air conditions and solid desiccant levels of moisture saturation [10–12,14]. Since they do not provide sensible cooling, a sensible cooling device must be added to the dehumidification system.

Desiccant wheels are rotating wheels with air channels coated with desiccant materials. While humid air flows through the process air channels, the desiccant material on one angular section (close to half of the circle) of the rotating wheel adsorbs the air's moisture. In Fig. 3b, the dehumidification section is shown in the lower section of the wheel. Meanwhile, the upper section is dedicated to regeneration. Meanwhile, the desiccant material on the rest angular section is regenerated/dried by the hot, dry air through the regeneration air channel, which is parallel to the process air channel, but in the opposite direction. The DW with relatively simple mechanisms can provide a continuous supply of dehumidified air with simple operation and controls. The dehumidification performance of the DW is influenced by its rotational speed [15] and channel size and depth. Moisture Removal Capacity (MRC) represents the total amount of moisture from the air removed by the device. Equation [1] shows MRC as a function of process air mass flow rate ($\dot{m}_a$), air humidity at the inlet ($\omega_{in}$) and air humidity at the outlet ($\omega_{out}$). The optimal rotational speed for *MRC* depends on outdoor humidity, regeneration temperature, and area ratio between dehumidification and regeneration sections [16,17]. DW has some drawbacks that limit its application. These wheels must be of large volume relative to the processed airflow to obtain a significant amount of dehumidified air due to the adsorption heat released during the adsorption process, which reduces the absorption capability of the desiccant material. To provide sensible cooling, they can be integrated with direct or indirect evaporative cooling or vapor compression systems [18].

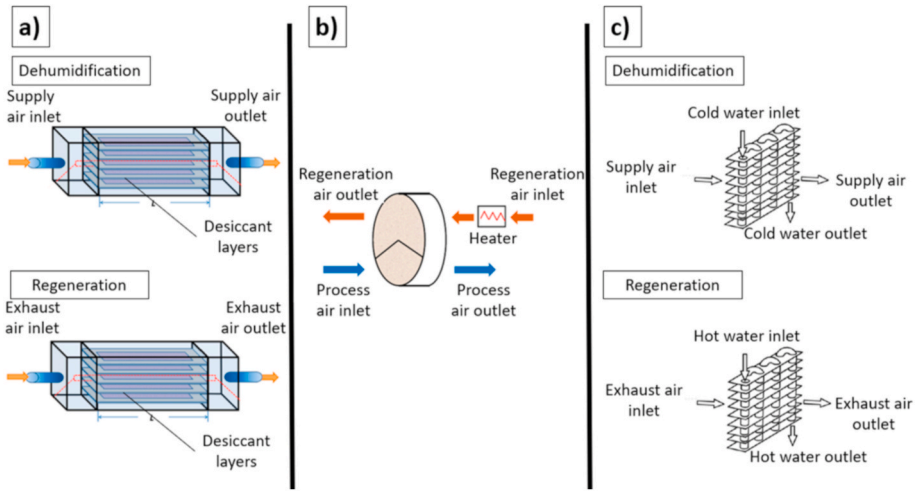


**Fig. 3.** Solid desiccant dehumidification devices. a) fixed bed [22], b) desiccant wheel [23], c) DCHE [19]. [reproduction].

$$MRC = \dot{m}_a(\omega_{in} - \omega_{out}) \quad (1)$$

The third type, the DCHE, as developed by Ge et al., 2010 [19], evolves from previous designs of desiccant-coated cross-flow plate heat exchangers cooled by air. DCHE was improved on that design by replacing air with water as a cooling fluid. DCHEs are solid desiccant material coated fin and tube heat exchangers. Fig. 3c shows the cross flows of air and water and the disposition of solid desiccant material over the fins of the DCHE. By using internal cooling, the DCHE can reject the adsorption heat to the cooling water. Thus, the DCHE can maintain a near-isothermal dehumidification process to reduce the devices' irreversibility. Managing the cold-water temperature can avoid an increase in air temperature and provide sensible cooling to the process air. The lower operation temperature Experimental studies show that MRC depends on the regeneration temperature [19]. However, increasing the regeneration temperature increases the heat losses from the DCHE to the surrounding ambient due to the increase in temperature difference [20], so a compromise between both conditions must be reached.

As fixed-bed devices DCHE presents an alternative operation, requiring at least two devices working parallel to provide a continuous dehumidified airflow [21]. The dehumidification-regeneration cycle length depends on the ambient conditions, design, and materials of the DCHE and water mass flow rates and temperatures. Therefore, the cycle time shows significant variations and duration of dehumidification and regeneration processes [20].

A DCHE device requires cold water during the dehumidification process and hot water during the regeneration process. To provide either fluid, the DCHE must be connected to supply loops for each. The control system can direct the required fluid to the DCHE at each process by using fluid valves. On the airside, a similar variable loop is needed. The air out of the dehumidifier is further cooled by an auxiliary sensible cooling device (if required) and then delivered to the building. On the other hand, the regeneration air can either be exhaust air from the building or drawn directly from outdoors during the regeneration process. The air loop must change the source and destination of the air that blows through the DCHE by using a series of dampers directed by the control system. The control system must coordinate the water and air loops of the DCHE for the alternative processes. Therefore, at least two DCHE devices must work as a relay to provide continuous dehumidification and be regenerated consequently. Correspondingly, the hot and cold water sources, the valves, and dampers of the DCHE connections will switch continuously to direct the fluids to the required DCHE unit according to the process being performed at each at any instant.

### 2.3. DCHE deployment

Continuous operation of cold and hot water sources is required to maintain two or more DCHE devices' continuous operation. The hot and cold water temperatures will vary according to the operational conditions and materials selected for the DCHE. These temperatures of cold water and hot water can be around 15 [C] and 50 [C], respectively [24]. Common HVAC devices can provide them. Given the development stage of this technology, several aspects of it are being investigated through laboratory-scale prototypes. Full setups of DCHE-based dehumidification systems are built and studied [3,20,25–29]. Also, a partial setup for DCHE design is analyzed [30]. Possible system configurations using DCHEs for dehumidification are studied both experimentally and numerically [21,25,31]. In these studies, the hot water mainly from solar thermal collectors [21,25], and auxiliary heating sources are used for the regeneration power. Either evaporative coolers [25] or cooling towers [21,31]have been used to remove the absorption heat. Bidirectional fans provided airflow for the dehumidification and regeneration processes. Meanwhile, water valves directed hot and cold water to the DCHE units performing regeneration or dehumidification, respectively. Additional improvements in these configurations include the use of additional sensible heat exchangers in different system locations. An additional heat exchanger can be deployed between the DCHE and the building to provide additional cooling before supplying dehumidified air into the building [26]. Also, an additional heat exchanger can be located between the DCHE and the exhaust of regeneration air to recover part of the heat transferred to the air during the regeneration process [27]. These modifications allow to increase the degree of control over the supplied air temperature or reduce the system's energy consumption, respectively.

For testing purposes, experimental setups include the following components: climatic chambers to provide inlet air at temperature and humidity resembling the desired outdoor conditions [20,28]. Process and regeneration air loops include fans with variable speed drives [3,30]. For the waterside, hot and cold water are generated in thermostatic baths [3,28,30] or in a vapor compression system [29], and then two independent circuits for hot or cold water direct each fluid to the corresponding DCHE at each cycle.

For the successful commercial application of DCHE, reliable system configurations must be developed. However, the present review focuses on the design and materials of DCHE devices. Therefore, DCHE deployment as part of a dehumidification and air conditioning system was presented briefly only to provide the necessary context, and no further discussions of alternative system configurations or system-level energy performance are included.

## 3. DCHE materials

Materials used in DCHE include solid desiccant materials, substrate, binders, and heat exchanger structure materials. The substrate and structure materials must have high thermal conductivity, like aluminum or stainless steel, to maximize the heat transfer between the air and the solid desiccant [32]. Aluminum is often used as a substrate in DCHE due to its high thermal conductivity and lower cost compared to copper [33]. The materials used in both DCHE and novel heat exchanger designs are reviewed below.

### 3.1. Substrate materials

Substrate materials provide structural integrity and strength to the heat exchanger [32] and mechanically support the solid desiccant material.

#### 3.1.1. Metal foams

An alternative to metallic fins is metal foam with a higher coating surface area than conventional aluminum fins [33]. A high surface-to-volume ratio allows deploying a larger surface of solid desiccant material in contact with the airstream. Since the water adsorption by solid desiccant materials is a surface phenomenon, a higher surface of solid desiccant material can improve dehumidification performance.

Substrate materials with high thermal conductivity allow conducting heat generated by the exothermic adsorption process away from the solid desiccant. This way, solid desiccant can be kept at a lower temperature, sustaining the adsorption process for longer periods. Aluminum has a relatively high thermal conductivity, for which it has seen widespread use as the substrate material. However, the bulk properties of aluminum in metal foam form differ from those of solid aluminum. Aluminum metal foam presents a low bulk thermal conductivity compared to solid aluminum (2–7 [W/mK]) due to the large volume of voids filled with air in the foam.

To thoroughly characterize the metal foams for heat exchangers, some researchers measured heat transfer coefficient and pressure drop for different aluminum foams, classified by their Pore Per Inch (PPI). They found that the airside heat transfer coefficients and pressure drop values also increased by increasing the PPI. Airside heat transfer coefficients for 40 PPI aluminum foam reached 400 [W/m2K], twice as compact fin and louver heat exchangers at the same flow conditions [34]. This increase in airside heat transfer coefficient is due to its highly irregular structure, promoting turbulent flow.

#### 3.1.2. Graphite

Researchers have studied graphite as an alternative to metal for flat-plate heat exchangers plate to its high thermal conductivity and lower weight [35,36]. The use of graphite plates requires the use of adhesives to bind the plates because the usual brazing process for metallic plates cannot be used in the graphite plates [35,36], and pre-oxidization can improve desiccant fixing into the plates [36].

### 3.2. Solid desiccant materials

Desiccant materials are adsorbent, highly porous materials with a high surface area per volume unit. Commonly used solid desiccant materials include silica gel, zeolites, hygroscopic salts, metal-organic frameworks, etc.

Relevant properties of desiccant materials for dehumidification are the maximum moisture content uptake, water adsorption isotherm curves, and thermal conductivity. The equilibrium water adsorption of desiccant materials can be represented in the adsorption isotherm curves, which show the maximum moisture uptake of the desiccant material relative to the moisture content capacity as a function of relative pressure. Adsorption isotherm curves of different desiccant materials have been classified into eight types by the International Union of Pure and Applied Chemistry (IUPAC) [7], as shown in Fig. 4. The adsorption and desorption processes in DCHE take place at relative humidity values between 30 % and 80 % [24], which have been highlighted in the areas between the dashed lines of Fig. 4.

Type IV and V show hysteresis loops in Fig. 4, which indicate the irreversible transitions between desorption (regeneration) and adsorption (dehumidification). The direction of the upper-right arrows indicates the adsorption process, and the lower-left arrows indicate the desorption process. The characteristics of each hysteresis loop are due to the specific combination of pores of different sizes in each material. The presence of hysteresis is related to the condensation process inside the pores. During the desorption process, either the condensate inside the pore is stable, or the entrances of the pores are blocked so that the condensate cannot flow with the airstream. Therefore, after the desorption, a certain amount of condensate remains inside the solid desiccant material. For the following adsorption cycle, those pores will not be able to capture moisture from the humid airstream, being already occupied by condensate particles, thus reducing the device's maximum moisture uptake capacity. Fig. 5 shows six types of hysteresis loops of solid desiccant materials defined by IUPAC [7].

Therefore, the most convenient adsorption isotherm and the least detrimental hysteresis loop (if any) would present a high moisture content increase in that range for the adsorption (dehumidification) process and high moisture content reduction in the same range for regeneration. If the isotherm adsorption curve presents most of the increase in moisture content at high relative humidity values, the DCHE will not dehumidify the air down to comfort levels unless air humidity reaches high values. Suppose the increase in moisture content shown by the adsorption isotherm takes place at lower relative humidity values. In that case, the material will saturate before dehumidifying the air down to comfort levels. Similarly, for the regeneration process, if most of the reduction in moisture content takes place at low values of relative humidity, it would be necessary to provide excessive heat to regenerate the material. Then, the better-suited adsorption isotherm curves for DCHE are types V, IV, and II, in order of preference (Fig. 4). Meanwhile, from the hysteresis loops shown in Fig. 5, H2(a) and H2(b) would be the least detrimental to DCHE operation.

According to their structure, solid desiccant materials can be classified as nanoporous organic materials, composite materials, and polymeric materials [4].

#### 3.2.1. Nanoporous inorganic materials

Nanoporous inorganic materials encompass solids with pores ranging between 0.2 [nm] to 50 [nm]. According to their composition, nanoporous inorganic materials can present different levels of water adsorption capacity, regeneration temperature, or even different water adsorption isotherm curves. Materials like aerogel and Aluminophosphates (AlPO) molecular sieves are in this category.

Aluminophosphates (AlPO) molecular sieves have type V (the favorable type) adsorption isotherm curves [6,37–39] but differ from zeolite materials with a similar molecular structure whose behavior is more akin to type-I curves [4]. However, the materials present hysteresis at low relative pressure after been exposed to two adsorption-desorption cycles [39]. The application of AlPO materials in desiccant wheels compared to pure Silica Gel based devices [37], but for the possibility of using low-temperature heat (333 [K]) of regeneration as a potential advantage for the use of zeolites [38].

Aerogels are good candidates for solid desiccant applications due to their high specific surface [4]. They can be manufactured from precursors such as silica, alumina, titania, and zirconia. The adsorption characteristics of silica aerogel for dehumidification applications have been experimentally studied [32]. Aerogels showed a type V adsorption isotherm curve and showed stable adsorption characteristics for up to 25 adsorption-desorption cycles. The water adsorption isotherms and behavior after being exposed to several adsorption-desorption processes

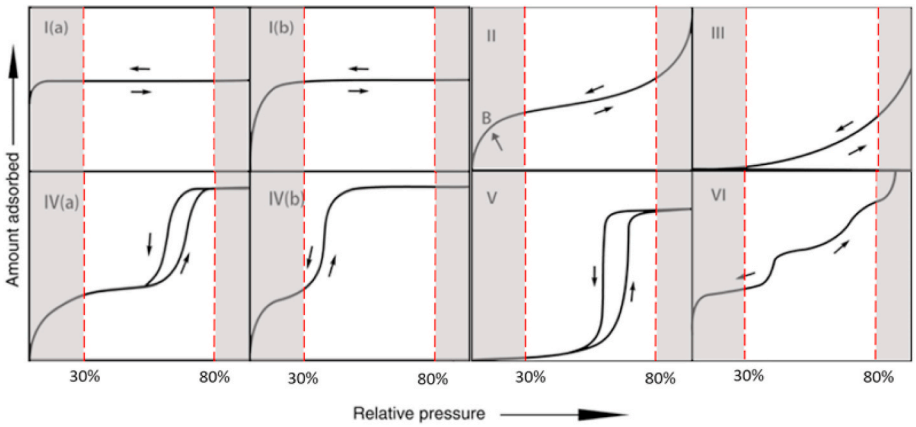


**Fig. 4.** IUPAC adsorption isotherm curves classification, adapted and modified [7].

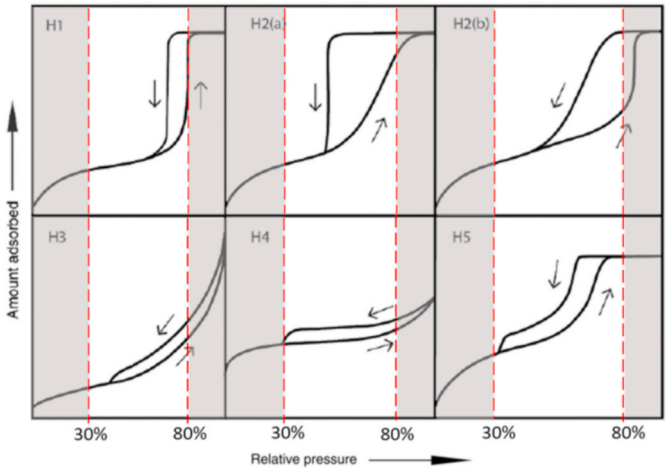


**Fig. 5.** IUPAC hysteresis loops classification, adapted and modified [7].

of different types of aerogels were studied [40]. All samples showed a noticeable increase in moisture content from relative pressure values from 0.8 upwards.

### 3.2.2. Composite desiccant materials

Composite desiccant materials use porous matrix materials, in which a secondary material embedded can increase its water adsorption properties. A typical example is hygroscopic salts, such as lithium chloride (LiCl) and lithium bromide (LiBr), on silica gel or carbon matrixes. During the adsorption process, hygroscopic salts present a lyolysis process, and the airflow drags salt particles into the supply airstream. By employing a matrix material, degraded salts are not dragged by the airstream and remain confined inside the host matrix. Still, the high affinity of the salts with the water vapor particles increases the moisture uptake capacity of the composite materials.

Biopolymer Chitosan (CS) was studied as a matrix material, using mesoporous silica (SBA-15, MCM-41), mesoporous carbon (MC) [41], and non-lyophilic salts (boehmite - AlOOH) particles [42]. The adsorption isotherm curve shape of CS-AlOOH composite has been identified as Type III, whereas the curves of CS-SBA-15 and CS-MC as Type IVa and CS-MCM-41 as Type IVb. CS-AlOOH samples were subjected to 10 adsorption-desorption cycles, and total regeneration was found at 15–20 min for 80 °C and 10–15 min for 100 °C. CS-SBA-15 reached 1.37 [gr water/gr adsorbent] adsorption capacity and CS-AlOOH reaches 1.5 [gr water/gr adsorbent], both higher than pure CS which reaches 1.3 [gr water/gr adsorbent], but CS-MCM-41 and CS-MC presented lower values than non-treated CS (1.21 [gr water/gr adsorbent] and 1.29 [gr water/gr adsorbent], respectively). The use of composite materials based on metal-organic frameworks (MOF) has also been studied [43,44]. The studied material has a MOF-based matrix (MIL-101) and incorporates graphite oxide (GO) in it to increase its water sorption capabilities. Several versions of the MOF composite were synthesized and characterized [44], by varying the weight fraction of graphite oxide contained in it. The sample with a 6 % weight/weight of graphite oxide showed the highest water vapor capacity. It was used for adsorption-desorption cycles testing and found to have a stable behavior.

A composite desiccant material based on polyvinyl alcohol (PVA) and different concentrations of lithium chloride was developed and characterized [45]. To avoid lyolysis, LiCl content was limited to 50 % on weight. The authors found that for 80%RH, PVA-LiCl (50w%) presented an equilibrium sorption capacity of 177.2 %, whereas SG only reached 28 % for the same conditions. For the operational test with DCHE, the author found that both materials produced a similar final level of dehumidification of the process air. Still, the PVA-LiCl DCHE saturated slower than the SG DCHE, which provided a larger amount of dehumidified air before the DCHE required regeneration (see Table 1).

### 3.2.3. Polymeric materials

Among polymeric materials, Metal Organic Frameworks (MOF) have been intensely and widely studied as desiccant materials due to their promising water adsorption characteristics. Thus the review on the polymeric material group is focused on MOFs. MOF materials, which are polymeric, microporous crystalline materials, are attractive as solid desiccant materials due to their high surface area and moisture uptake capacity. Materials such as MIL-100 [46], MIL-160 [47], MOF-801 [48] and Cr-soc-MOF-1 [49] have been analyzed and showed water vapor uptakes as high as 1.95 [gr/gr] at 70 % relative humidity (Cr-soc--MOF-1). No noticeable hysteresis or degradation of the material during the tests has been found [48,49]. Also, the performance of MOF as desiccant materials on adsorption cooling and dehumidification applications has been studied and compared to traditional desiccant materials [46,50]. After obtaining MIL-100 (Fe) adsorption characterization, the authors simulated it for passive moisture control in buildings to reduce the latent cooling load and compare its performance to laminated wood. It was found that MIL-100 (Fe) produced better moisture control during the day, and it could be regenerated passively while using night ventilation only by releasing the adsorbed moisture to lower relative humidity air. A simulation of the operation of desiccant wheels using aluminum fumarate or silica gel as desiccant material showed that aluminum fumarate reached higher dehumidification capacity. Still, the lower mass of adsorbate was removed than silica gel [50]. Table 2 shows the reviewed solid desiccant materials, indicating maximum moisture uptake, adsorption isotherm curve types, and relevant findings.

**Table 1**
Features of different solid desiccant-based dehumidification devices.

| Technology | References | Advantages | Disadvantages |
|---|---|---|---|
| Desiccant wheel | [15–18] | Continuous supply of dehumidified with only one device; Simple mechanical and control systems than DCHE; A high degree of control of the process (rotation speed, regeneration temperature, and airflow) | Low desiccant material utilization due to temperature increase, leading to large volume devices; Require additional sensible cooling devices; May require splitting the process into several stages to reduce regeneration temperature, requiring more than one DW in each stage |
| Fixed bed | [10–14] | Simple mechanical design; Low maintenance | Low desiccant material utilization due to temperature increase, leading to large volume devices; Limited level of control over the process; Require additional sensible cooling devices; Highly variable, non-controllable outlet conditions; Require two parallel devices for continuous dehumidified air; High-pressure drops (packed bed design) |
| Internally cooled – Desiccant coated heat exchangers | [19–21] | High desiccant utilization due to controlled dehumidification temperature; Sensible and latent cooling is possible in the same device; The high degree of control of the process (hot/cold water temperatures and mass flow rates) | Require two parallel devices for continuous dehumidified air; Complex control and mechanical system |

#### 3.2.4. Long term solid desiccant materials stability

Given the cyclical nature of DCHE operation, solid desiccant materials are exposed to temperature changes and adsorption and desorption processes. These conditions generate stress over the material due to thermal expansion and contraction and also due to the binding and release of water molecules to and from the desiccant microstructure [47]. Therefore, it requires not only favorable water sorption uptake, isotherm, and kinetics but also long-term material and performance stability.

In composite materials, including hygroscopic salt particles, the maximum salt content is limited by the onset of lyolysis [6]. By increasing the salt content, water adsorption uptake can be improved, but at the risk of releasing salt particles from the solid desiccant into the airstream. This way, the salt content and, therefore, water adsorption uptake of the material reduces. Therefore, the salt content must be kept at a level that limits lyolysis and salt particle carryover at the expense of higher water adsorption capacity [45].

Regarding MOF materials, despite their high porosity and water adsorption capacity, initial developments produced materials that degrade with water. Therefore, the development of these materials for dehumidification has centered around increasing their stability when exposed to water molecules. A solution to this problem has been the use of chromium-based MOFs, whose microstructure can withstand capillary forces that take place during desorption [49].

Despite the relevance of ensuring long term stability of desiccant materials, the characterization of solid desiccant materials tends to focus on a low number of cycles (6–100 cycles [42,44,49,50]) for hysteresis analysis, rather than long term stability.

### 3.3. Binders

Binder materials must be added to the solid desiccant to ensure the mechanical adhesion of the solid desiccant coating layer on the substrate surface [6,51–53]. The researchers studied the binder materials between silica gel/zeolites and metallic substrates, including graphite powders, metallic foams, polyaniline, polyvinyl alcohol (PVA), aluminum hydroxides ($AlOH_3$), and polytetrafluorethylene (PTFE) [6]. Also, epoxy, PVA, corn-flour, hydroxyethyl cellulose (HEC), gelatin, bentonite, and sepiolite with silica gel (type 3A and type RD) over aluminum plates were tested [51]. Trimethoxypropylsilane was used as a binder for SAPO-34 and FAPO-34 zeolites over aluminum [54], Polysiloxane has been used as a binder for MOF material (microporous aluminum fumarate) over aluminum plates [55], PVA was used as a binder for silica gel over a stainless-steel substrate [56] and for AlPO-18 zeolite over aluminum plates ($AlMg_3$ alloy, over 94 w% aluminum) [53].

Incorporating a binder material into the interparticle spaces of solid desiccant materials improved heat transfer by increasing the physical contact inside the porous structure. It also reduced mass transfer capacity due to pores obstruction [51,52]. The use of HEC binder at 3.3 w % with type 3A silica gel over aluminum causes a reduction in maximum water uptake from 0.43 [gr/gr] to 0.356 [gr/gr] [51]. In the case of SAPO-34 and FAPO-34 zeolites using Trimethoxypropylsilane as the binder material, the maximum water uptake was reduced between 5 % and 10 % [54], and the BET surface area by 6 % and 13 %, respectively. Nevertheless, the use of PVA as the binder for silica gel did not significantly reduce the BET surface area, pore-volume, nor sorption kinetics [56]. Fig. 6 shows the effect over porous volume and surface area of different concentrations of the mixer (HEC) in silica gel solid desiccant. It can be seen by increasing the concentration of binders, both porous volume and surface area are reduced. This reduction minimizes the moisture uptake capacity of the solid desiccant.

The binder influences the mechanical resistance of the desiccant layer. The use of inorganic binders (Bentonite and Sepiolite) and organic binders such as gelatin and PVA with silica gel over aluminum plates showed limited fixation, and even peeled off was observed. However, the HEC binder showed good fixation over the aluminum plates [51].

The selected binder material must be chemically inert to the solid desiccant and water pair [51]. The regeneration temperature must not produce degradation on the binder material. In the case of PVA, this starts degrading at 200 °C and therefore is adequate for use in DCHE [56]. Table 3 shows different combinations of binder material, solid desiccant, metallic substrate, and relevant findings.

## 4. DCHE design

The following section reviews different geometrical configurations of both uncoated heat exchangers and solid desiccant-coated heat exchangers. Even though DCHE is made from existing heat exchangers, the designs of already developed DCHE are presented in the DCHE subsection. Another subsection titled 4.2, "Prospective desiccant coated heat exchangers design," reviews designs of heat exchangers that have not been tested for their use as DCHE, but their performance or geometric characteristics make them good candidates for DCHE use.

A common design for the DCHE are fin and tube heat exchangers [19,21,27,28,55,57]. This configuration presents a commercially available design. However, in the cited studies, no mention of the reasons to use fin and tube heat exchangers instead of alternative designs is presented. Next, new possible designs of heat exchangers are discussed. Six different designs of heat exchangers reviewed are shown in Fig. 7 a) represents finless tube heat exchangers and a close view of the finless

**Table 2**
Solid desiccant materials characteristics.

| Type | References | Materials | Maximum water uptake [kg/kg] | Adsorption isotherm curve | Additional notes |
|---|---|---|---|---|---|
| Nanoporous inorganic material | [6,37–39] | AQSOA Z01, Z02, Z03, Z05 Zeolites | 0.2–0.33 | Type V | Specific heat 0.94 [kJ/Kg-K]. Pore diameter 0.73 [nm]<br>AQSOA 01: Saturation at 6000 [s], 0.2 [kg/kg], 298 K<br>AQSOA 02: No saturation at 15000 [s], 0.24 [kg/kg], 298 K<br>AQSOA 05: No saturation at 4000 [s], 0.18 [kg/kg], 298 K |
| Nanoporous inorganic material | [32,40] | Silica, Alumina, and mixed salts aerogels | 1.15–1.35 | Type V | Water mass diffusion coefficient 0.89 × $10^{-10}$ [$m^2$/s] (potassium hydroxide); 13.74 × $10^{-10}$ (hydrogen peroxide) [$m^2$/s] |
| Composite material | [41,42] | Chitosan based composite | 1.21–1.5 | Type III-Type V | Regeneration temperature 80 °C<br>Total desorption from 1.5 [kg/kg] in 15–20 min at 80 °C |
| Composite material | [43,44] | MIL 101 with graphite oxide composite | 1.58–1.6 | Type V | MIL101 matrix with 6 % w/w graphite oxide. Langmuir surface area 5188 [$m^2$/g]<br>Saturation at 6600 [s], 1.5 [kg/kg], 298 K, 70%RH |
| Composite material | [45] | PVA-LiCl Composite | 1.77 | Type II | A higher concentration of LiCl presented higher adsorption capacity, but to limit deliquescence concentration was limited to 50%w. Regeneration temperature of 40 °C<br>No saturation at 30000 [s], 1.75 [kg/kg], 303 K, 80%RH |
| Polymeric | [46] | MIL-100 (Fe) | 1.6 | Type V | Steep adsorption region between 25 and 50 % |
| Polymeric | [47] | MIL-160 | 0.4 | Type V | 90 % of uptake happens at 20 % RH. Thermal conductivity 0.061 [W/m-K] at 25.4 °C |
| Polymeric | [48] | MOF-801 | 0. | – | Specific area 900–820 [$m^2$/g]. Pore volume 0.49–0.44 [$cm^3$/g]<br>Saturation at 300 [s], 1 [kg/kg], 308 K |
| Polymeric | [49] | Cr-soc-MOF-1 | 1.95 | Type V | Adsorption capacity maintained up to 100 cycles. Apparent surface area 4549 [$m^2$/g] |
| Polymeric | [50] | Aluminum fumarate | 0.45 | Type V | No loss of water uptake capacity up to 40 cycles |

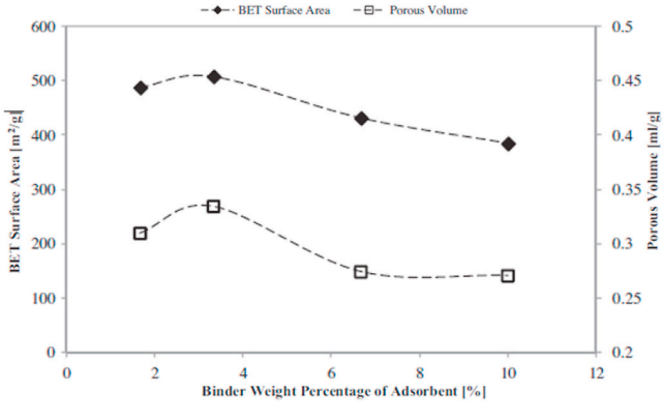


**Fig. 6.** Effect of binder concentration over porous volume and surface area [51].

teardrop-shaped tubes [58], b) shows a wire and tube heat exchanger [59], c) shows a metal foam heat exchanger [60], d) presents the pieces to assemble a graphite plate heat exchanger [36], e) presents a micro-channel heat exchanger and shows a close-up image of the corrugated fins before and after coating with a solid desiccant material [61], f) shows a lattice heat exchanger [62], with internal water tubes.

### 4.1. Desiccant coated heat exchangers design

#### 4.1.1. Fin and tube heat exchangers

The effects of fin depth and fin pitch over dehumidification performance have been studied. Shorter depth fins with smaller pitches presented the highest heat transfer coefficient and the highest moisture uptake than the larger fins and pitch designs, even by 19 % and 18 %, respectively [3]. However, this heat and mass transfer improvement was at the expense of a higher pressure drop, even up to 90 % higher than less compact designs. Other works also studied the effect of fin length over dehumidification performance, finding that doubling the length of the fins increased MRC by 40 % [63].

Additively manufactured new fin designs have been tested to increase the heat transfer rate [64]. The designs aim to increase conduction heat transfer on the fin and convective heat transfer between the fin and the exterior fluid. The authors tested two designs of fins by varying the Reynolds number on the channel and the spacing between fins and compared them to a simpler circular fins design. It was found that circular integrated pin fins and serrated integrated pin fins reached higher Nusselt numbers than the plain fin design and that the highest volumetric flux density with a value of 2.72 [kW/$m^3$K] was found for circular integrated pin fin. Additionally, the authors developed empirical correlations for Nusselt, Reynolds, and Prandtl numbers as functions of fin spacing and design from the data measured in the experiments. The authors found that the fin efficiency of the new models was lower than

**Table 3**
Binder, solid desiccant materials, and substrate sets.

| Reference | Solid desiccant | Substrate | Binder | Relevant findings |
|---|---|---|---|---|
| [51] | Silica gel (Type 3A, Type RD) | Aluminum | Polyvinyl Alcohol | Peel-off observed |
| | | | Hydroxyethyl cellulose | 17 % reduction in maximum water uptake (Type 3A) |
| | | | Gelatin | Peel-off observed |
| | | | Bentonite | Limited fixation |
| | | | Sepiolite | Limited fixation |
| [54] | SAPO-34 Zeolite | Aluminum | Trimethoxypropylsilane | 5 % reduction in maximum water uptake, 6 % reduction in BET surface area |
| [54] | FAPO-34 Zeolite | Aluminum | Trimethoxypropylsilane | 10 % reduction in maximum water uptake, 13 % reduction in BET surface area |
| [55] | Microporous aluminum fumarate | Aluminum | Polysiloxane | No issues regarding binder performance |
| [56] | Silica gel | Stainless steel | Polyvinyl Alcohol | No significant reduction in BET surface area, pore volume, nor sorption kinetics |
| [53] | AlPO-18 Zeolite | Aluminum (AlMg3 alloy) | Polyvinyl Alcohol | Sedimentation between large size desiccant particles and binder particles closer to the surface |

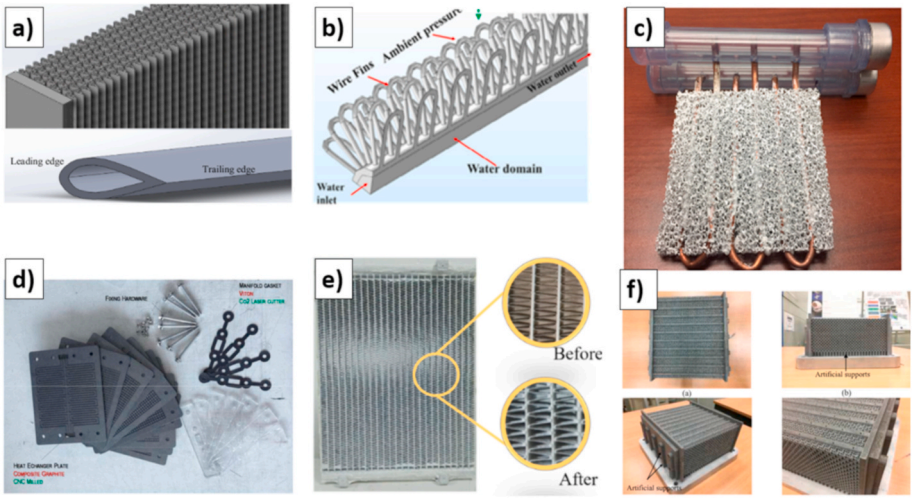


**Fig. 7.** Heat exchangers designs reviewed. a) Finless tube [58], b) wire and tube [59], c) metal foam [60], d) graphite plate [36], e) microchannel [61], f) lattice [62].

that of plain circular fins due to higher convective heat transfer. However, considering the performance evaluation criterion (ratio between heat transfer and flow resistance), the new fin model designs showed improved performance over traditional fins.

#### 4.1.2. *Wire and tube heat exchangers*

Wire and tube heat exchangers are devices in which the usual fin surfaces used to increase the heat transfer area of the airside are replaced by wires or wire fabric. This way, the heat exchangers do not present fins at all, and the air flow takes place through the wire mesh outside the water tubes.

The performance of wire heat exchangers has been studied and compared numerically and experimentally to finned and microchannel heat exchangers [65]. The heat exchangers were coated on aluminum fumarate, a MOF solid desiccant material, and tested for pressure drop, water uptake, and temperature distributions. The wire heat exchanger showed lower pressure drop and better heat transfer performance than microchannel and finned exchangers by comparing their fin temperatures and pressure drop. Microchannel and wire heat exchanger reached 91 °C at 700 s of simulation, whereas the rectangular fins heat exchangers reached 71 °C. However, the microchannel reached four times higher water side pressure drop than the wires heat exchanger. Therefore, wire spacing, wire height, and tube diameter were optimized to improve thermal performance and water uptake, finding that 1 [mm] spacing between wire sections produced higher water uptake during the 1800 s of dehumidification process simulation.

A tube-based wires heat exchanger with polymer tubes and outer metal wires has been developed [59]. In this configuration, the metal wire transfers heat by conduction between the sections inside the tube in contact with the liquid and the sections outside it, in contact with the cooling gas. Additionally, the presence of the wires distorts the flow of both fluids, creating turbulence and therefore increasing the convective heat transfer between the fluids and the wires. The authors built a prototype with ABS polymer using additive manufacturing and experimentally measured its heat transfer performance. Later, they compared the measurements from the prototype with the performance of fin and tube heat exchangers from the literature. The prototype heat exchanger showed higher (220 % and 125 %) heat transfer to weight and volume ratio, respectively, compared to fin-tube heat exchangers with the same ratio of heat transfer rate to pumping power.

A comparison of wire meshes heat exchangers with a metal foam and a bare tube heat exchanger showed that the wire mesh heat exchanger reached higher Nusselt numbers than the metal foam heat exchanger, and both were higher than the bare tubes heat exchanger [66]. Especially, a 28 % increase in Nusselt number compared to a metal foam heat exchanger was found after the characterization of both heat exchangers. When using metal foam, the main improvement in heat transfer performance is due to the fin effect. For this reason, the method for joining the metal foam to the tube becomes relevant. In the case of wire meshes, the increase in performance is due to increased turbulence on the airside, so they are not as sensitive to joining methods as metal foams [66].

A wire fabric consisting of low and high wire densities sections and then assembled to form a wire and tubes heat exchanger has been studied [67,68]. The higher density areas were placed in mechanical contact with the tubes. Meanwhile, the lower density areas were exchanging heat with the fluid. It was required to develop detailed models of the wire fabric using commercial CFD software due to the lack of empirical correlations. These simulations showed that the number of transfer units of the wire heat exchanger was 1.5 times higher than that of a louvered fin heat exchanger for comparable friction factors. Also, by reducing the lateral distance between wires, the friction factor increased significantly [67]. The following study included experimental testing of wire heat exchangers in addition to the numerical simulations of flat tube wires, mesh heat exchangers, and round tube wire meshes heat exchangers [68]. The experiments considered small samples of wire fabric for testing for pressure drop and heat transfer. The experimental wire heat exchangers showed lower performance than predicted by the simulation and the reference heat exchangers. However, it was due to imperfect thermal contact between the wire fabric and the tubes in one case. Wire fabric heat exchangers showed 1.2 to 2 higher mass efficiency than the reference heat exchangers. Then, for the same mass, and by having higher air surface area, wire mesh heat exchangers present higher heat transfer performance for the same mass than fin heat exchangers.

#### 4.1.3. *Microchannel heat exchangers*

The performance of microchannel and fin and tube desiccant coated heat exchangers has been compared [69]. Microchannel heat exchangers are characterized for reaching higher heat transfer performance than traditional fin and tube heat exchangers (For Reynolds number from 80 to 480, Microchannel Nusselt number from 9 to 20.5, and for fin and tube 4.2 to 10.2), but at higher pressure drops due to the reduced channel size (125 % higher pressure drop per unit area in Microchannel heat exchanger as compared with fin and tube heat exchangers). Their higher heat transfer performance makes them suitable for solid desiccant applications. Both heat exchangers were coated on silica gel solid desiccant. After the coating process, the mass transfer

coefficient of the microchannel heat exchanger is also higher than the fin heat exchanger by 15 %.

#### 4.1.4. Metal foam heat exchangers

The use of metal foam in heat exchangers has been the subject of several studies [30,34,60,70,71]. Metal foam solid desiccant-coated heat exchangers have been developed and studied [60]. Some authors have analyzed different assemblies between the metal foam and the tubes, indicating that the machining of the metal foam is a complex process that may affect the structural resistance of the foam [34,60]. For that reason, the tubes are placed in contact with the metal foam without machining through the foam. Metal foam-based heat exchangers were built and characterized based on their heat transfer rate and pressure drop, considering different porosity levels (5 PPI, 10 PPI, 20 PPI, 40 PPI) [34]. Additionally, the contact thermal resistance of three other methods for heat exchanger assembly was tested (thermal epoxy, thermal compound, and brazing), and estimated that brazing produced perfect thermal contact resistance and thermal epoxy reached a thermal contact resistance of 0.55 [$m^2K/W$]. At an air velocity of 6 [m/s], it was found that heat transfer rates up to 400 [$W/m^2K$] could be possible for 40 PPI metal foam heat exchangers. Commonly used correlations to determine the friction factor and Colburn factor j did not produce accurate predictions, and therefore the authors developed new empirical relationships with more accurate results from the experimental data. Other designs filled the voids of the metal foam with solid desiccant particles instead of coating its surface [30]. This configuration reached a specific cooling capacity, and moisture removal rate 3.5 and 2.5 higher than the metal-coated heat exchanger characterized but with a pressure drop 25 times higher.

The thermal performance of copper foam arrays has been tested for three porosity levels (10, 20, 30 PPI) [72]. The order of the porosities in the three sections influenced the thermal resistance of the array when tested with water as the cooling fluid (10-20-30 array behaved differently from 30 to 20-10 array). Other authors found similar results using air as the cooling fluid in plate heat exchangers with metal foam (20-30-60 PPI sections) filling the channels between the plates [73], indicating that a symmetrical design might not be the optimum for heat transfer.

A full-size metal foam heat exchanger was manufactured and experimentally studied, based on 10 PPI commercially acquired aluminum metal foam and copper tubes [70]. The metal foam was coated in copper by electrodeposition to allow a brazing process with the tubes to obtain good thermal contact. Small scale experiments on metal foam samples were performed to estimate the heat transfer performance of an entirely constructed metal foam heat exchanger. The experimental results of the characterization of the full-sized heat exchanger showed an increase of 13 % on the actual heat rejection by the heat exchanger compared with the estimations for a water mass flow rate of 0.4 [l/min], whereas, for 0.8 [l/min], the experiments showed 30 % less heat rejection than the estimations.

#### 4.1.5. Plates heat exchangers

Graphite is a suitable substrate material in heat exchangers due to its high thermal conductivity and lightweight (55–60 [W/mK] and 1900 [kg/m3], respectively). Therefore its use in plate DCHE has been evaluated [36]. On one side of the plate, solid desiccant (SAPO-34 zeolites) was deployed by either dip-coating or direct synthesis in different layout use of dip coating produced thicker solid desiccant layers (up to 200 [μm]). In contrast, direct synthesis allows us to obtain desiccant layers of tens of micrometers thick. Fluid channels are present on the opposite face of each plate. Two different channel layouts were numerically tested (parallel channel and mirrored double serpentine channels), choosing the mirror double serpentine layout for the construction of the prototype. Then, the graphite plates were assembled as a plate heat exchanger, and the use of epoxy resin and silicone as bonding materials was tested. Pressure and leakage tests were performed, and the silicone sample showed lower resistance to pressure and leakage.

### 4.2. Prospective desiccant coated heat exchangers design

#### 4.2.1. Finless heat exchangers

The performance of a compact tube heat exchanger has been experimentally measured [58]. The heat exchanger does not include fins in its design (bare tubes), and the transverse shape of the tube has been found through optimization in previous works. The use of fins increased flow resistance and reduced the heat transfer coefficient of the tubes due to the temperature gradients. Therefore the study of finless tube heat exchangers might provide solutions to those drawbacks. Based on the experimental results, the authors were able to generate Chilton-Colburn *j* and *f* power-law correlations based on Reynold's number for both wet and dry conditions tested.

#### 4.2.2. Lattice heat exchangers

Lattice heat exchangers are composed of repeating cells whose base is in contact with a heat source. They use the large exposed area of the lattice cells to reject heat via convection to the cooling fluid. The structure of the repeating cells acts as obstacles into the flow path that create turbulence and enhance convective heat transfer. Due to their complex geometry, additive manufacturing is used for manufacturing them. Lattice heat exchangers were compared to commercially available fin and tube heat exchangers based on their thermo-hydraulic properties [62]. Two different lattice heat exchangers were built, in which the size of their repeating cell varied (7 [mm] and 14 [mm] respectively), and therefore their airside surface area (2.204 [$m^2$] and 1.275 [$m^2$] respectively) and surface area to volume ratio (968 [$m^2/m^3$] and 470 [$m^2/m^3$] respectively) also varied. Lattice 1 presented a pressure loss per thickness unit 2.14 times higher than lattice 2. Lattice heat exchangers presented higher heat transfer coefficients than fin and tube heat exchangers but also created a higher pressure drop. Measured at the same pumping power per thickness unit, lattice heat exchangers presented a 45 % higher heat transfer coefficient than fin and tube heat exchangers. Forced convection in metal foam, corrugated and lattice structures have been numerically studied [71]. The Nusselt number under equal pumping power was compared. A new lattice structure was proposed based on its heat transfer properties (windward bend structure). All lattice cases studied presented higher heat transfer coefficients than the parallel flat plates, and also, as the airspeed increased, the difference in heat transfer coefficient increased between the different structures. The heat transfer coefficients ranged from 100 [$W/m^2K$] for 1 [m/s] up to 610 [$W/m^2K$] for 11 [m/s], and the tetrahedral lattice and metal foam presented the highest heat transfer coefficients. Meanwhile the plain channel showed values from 20 [$W/m^2K$] at 1 [m/s] up to 80 [$W/m^2K$] at 11 [m/s].

However, the increase in heat transfer coefficient also is correlated with an increase in pressure drop compared to the plain channel, with tetrahedral lattice and metal foam having the highest pressure drops at all tested velocities of 1800 [Pa] and 2300 [Pa] for 11 [m/s], respectively. Compared with the same pumping power, the Nusselt number of the metal foam is lower than other structures due to its high-pressure drop. The slanted pin structure with a lower heat transfer coefficient reaches similar values as metal foam and tetrahedral lattice when the pump power is taken into account. The new structure proposed (windward bend) reaches a heat transfer coefficient between 120 and 700 [$W/m^2K$] for airspeeds between 1 [m/s] and 11 [m/s] and has a pressure drop of 1320 [Pa] for air velocity of 1 [m/s], and reaches up to 1.2 to 1.3 higher Nusselt number than all the other designs evaluated. A tetrahedral lattice frame of different porosity levels for heat exchange was evaluated thermally and hydraulically using numerical simulations [74]. The model was validated experimentally using two types of additively manufactured lattice samples. Polymer samples were used for the hydraulic characterization, and 420 stainless steel and bronze samples were used for determining the Nusselt number. The simulations

showed that the lattice frame had a friction factor between 4 and 1.8 at a Reynolds number of 150 and 2.2 to 0.6 and a Reynolds number of 1000. The Nusselt number ranges from 31 to 82 for all Reynolds number and porosity levels simulated, similar to the values for metal foams.

## 5. DCHE manufacturing

The manufacturing of DCHE can be divided into two main sections: the manufacture of the substrate heat exchanger and the coating in solid desiccant material. The manufacture of the substrate heat exchanger follows the same process used for uncoated heat exchangers. The manufacturing process of fin and tubes heat exchanger is reviewed, along with the less common manufacturing processes of graphite plates heat exchangers and lattice heat exchangers, which requires using additive manufacturing. Regarding the solid desiccant coating process, two main processes are identified and reviewed. These processes consist of the direct growth of solid desiccant material over the heat exchanger surface and the heat exchanger coating with a layer of already formed solid desiccant material particles.

### 5.1. Heat exchanger manufacturing

Heat exchanger design is partly limited by the current state of their manufacturing methods. Fin and tube and metal foam designs rely on techniques such as tube expansion or brazing to provide thermal contact between the tubes and the fins. In the case of lattice heat exchangers, they rely entirely on additive manufacturing processes and specifically on selective laser melting (SLM) to generate metallic parts from metal powders. Next, a description of the most common manufacturing methods for the reviewed design of heat exchangers is presented, indicating their effects on the thermal performance of the heat exchangers.

#### 5.1.1. Fin and tube manufacturing

For the manufacturing of fin and tube heat exchangers, tube expansion processes and brazing processes are commonly used. Brazing involves the use of filler material between the tube and the fins. This filler material must present a lower fusion temperature than the rest of the components of the heat exchanger [75,76]. The assembled heat exchanger is introduced in a controlled atmosphere chamber and subjected to preset increasing temperatures, ranging from preheating up to the melting temperature of the filler. At this point, the filler material flows to the crevices of the assembly, filling up the gaps between the components and providing thermal and mechanical contact between the different pieces [76].

An alternative method to brazing is the expansion of the tubes in the preassembled heat exchanger [77–81]. A disadvantage of tube expansion processes is that gaps between the outer tube surface and the fins' inner face or collar face are created [80]. These gaps in the contact surfaces generate thermal contact resistances that increase the total thermal resistance of the heat exchanger [80]. However, this thermal contact resistance is often neglected during the design phase of the heat exchangers due to the difficulty of evaluating it [78]. The two main processes of tube expansion are hydroforming and mechanical tube expansion. The injection of high-pressure fluid produces hydroforming tube expansion into the tubes, increasing its diameter until reaching mechanical interference with the tube's inner perforation diameter [79]. Mechanical tube expansion is produced by the introduction of an expansion tool at the tube, whose outer diameter is larger than the initial tube diameter, and by being introduced into the tube, it plastically deforms and expands the tube until reaching mechanical interference with the fins, also deforming partially the fins tubes collar [79,80].

Different methods to manufacture metal foams, including open-cell metal foams used for heat exchanger manufacture, have been reviewed [82]. Metal foam has been used to improve the performance of two types of heat exchangers: tube-based [34,83,84] and plate heat exchangers [73,85,86]. In tube-based heat exchangers, the metal foam has been placed on the outside of the tubes to replace fins, and in plate heat exchangers, the metal foam has been introduced between plates. To manufacture these heat exchangers, two main methods to ensure the mechanical stability and thermal contact between the metal foam struts and the tubes or plates are used. One method is the use of adhesives for bonding [34,83,84] and the other is the use of brazing processes [34,85]. In the case of tubes heat exchangers, there are two methods for joining the metal foams with the tubes, either the machining of the metal foam using electric discharge machining method (EDM) [34,83]or wrapping the metal foam layer around the tube, and securing it in place using adhesive and exterior wire wrapping [84]. EDM has also been used for sizing metal foam segments for their use in plate heat exchangers [86]. As with fin and tube heat exchangers, the imperfect surface joint between the tube and the struts of the metal foam produces a thermal contact resistance that reduces the thermal performance of the heat exchanger [83,84]. This thermal contact resistance for bonded heat exchangers can reach values between 6 % and 69.9 % of the total thermal resistance of the heat exchanger, so the development of economically feasible and industrial level brazing methods for metal foams is highly encouraged by the authors [83,84].

#### 5.1.2. Graphite plates rolling

A process developed by Terrella Energy Systems Ltd has been described for generating graphite plates [35]. This process does not require expensive machining, as commercially produced graphite plates nowadays. Starting from graphite plates of density 120 [mg/cm$^2$], they were rolling pressed into 2 mm thickness plates and then cut and pressed to generate chevron patterns. Then, a resin impregnation bath was applied to seal the graphite pores. The perimeter male and female grooves of the plates were glued together to assemble the heat exchanger.

#### 5.1.3. Additive manufacturing

Additive manufacturing (AM) allows us to generate parts of complex geometry [59,64,87] and consolidates in one piece geometries that would require multiple components to be joined together by other manufacturing processes. Thus it reduces the risk of bad assemblies and leakage on the heat exchanger [87] and the thermal contact resistance between parts [64].

Selective laser melting has been used to produce heat exchangers [62,64,87,88]. The selective laser melting process must take place in an inert environment to avoid oxidation and combustion. Therefore the volume of the inert chamber sets a limit to the size of the part to produce [87,88]. Selective laser manufacturing has been used to produce microchannel and corrugated fins, hydraulic oil cooler heat exchangers, lattice heat exchangers, and annular fin and tube heat exchangers [62,64,87,88]. The layer size for these studies was between 30 [μm] to 50 [μm], with laser power ranging from 180 [W] to 400 [W].

Other models of heat exchangers have been manufactured using ABS tubes by the Fused Filament Fabrication (FFF) process, and a separate head to lay the metallic wires atop each polymer layer was needed [59]. The headers of the heat exchangers were manufactured separately using FFF and later joined to the tubes using epoxy adhesive. One limitation of this prototype is that the hot water temperature is limited to less than 105 °C due to the use of ABS polymer material. However, that value is significantly higher than the regeneration temperature range used in DCHE, which is between 50 °C and 70 °C [69]. Table 4 shows a summary of the different heat exchanger designs reviewed, including their base material properties, the manufacturing process required, and their surface area to volume ratio. Additionally, the table indicates if each heat exchanger design has been studied for use as DCHE.

### 5.2. Solid desiccant coating

Two conventional alternatives for solid desiccant coating are either the direct growth of solid desiccant material over the substrate or the

**Table 4**
Heat exchangers designs characteristics.

| Type | References | Surface area to volume [$m^2/m^3$] | Manufacture process | Base materials | Considered as DCHE | Additional notes |
|---|---|---|---|---|---|---|
| Finless teardrop tubes | [58] | 1089 | Additive manufacturing | Titanium | No | Chilton Colburn j and f correlations were developed for the HX geometry. Tested for wet and dry conditions |
| Wire and tubes | [59,65–68] | – | Parts assembly, additive manufacturing (Arie 2020) | Wires: Aluminum, copper, stainless steel. Tubes: Copper, ABS | Yes (Aluminum fumarate [65]) | Imperfect thermal contact between tubes and wires. Wire fins configuration affects performance |
| Microchannel | [69] | 929 | Parts assembly | – | Yes (Silica gel) | An increase in heat transfer is related to the increase in pressure drop, compared to fin and tube heat exchangers |
| Metal foam | [30,34,60, 70–73] | 739–1330 | Parts assembly | Foam: Aluminum, copper. Substrate: copper tubes, copper plate, aluminum plate | Yes (Silica aerogel [60], silica gel [89]) | Difficulties to drill tubes inside metal foam, alternative configuration proposed. Sequence of metal foam porosity affects heat transfer (tested array of 3 different porosity segments of metal foam) |
| Plates | [36] | 490 | Parts assembly | Graphite | SAPO-34 zeolite | Graphite plates cannot be brazed, tested epoxy resin and silicone for plates bonding |
| Lattice | [62,71,74] | – | Additive manufacturing | Aluminum alloy powder (AlSi10Mg), acrylic-based photopolymer (friction factor), stainless steel, and bronze (Nusselt number) | No | 0 |

coating of the substrate with a layer of already synthesized solid desiccant particles. Two methods are feasible to coat the substrate using already synthesized solid desiccant materials: dip coating and electrostatic spraying. The following section discusses coating of already synthesized materials and direct synthesis, and in the former category, dip coating and electrostatic spraying methods are presented and discussed.

### 5.2.1. *Coating of synthesized solid desiccant particles*

*5.2.1.1. Dip coating.* The use of dip coating of heat exchangers in a binder and solid desiccant particles solution is a common procedure to obtain DCHE devices [54,89–95]. The general procedure consists of the preparation of the binder and solid desiccant solution, covering the surfaces with the solution, and later curing the coated surfaces to ensure adhesion of the desiccant layer. Aspects of the procedure vary according to the desiccant materials and binders used. In the case of zeolite coating of aluminum sheets, degreased aluminum sheets were submerged in zeolite solution for 2 min. After removing the sheets from the solution, the aluminum sheets were cured at 120 °C for 4 h [54]. To manufacture silica gel-LiCl composite solid desiccant aluminum coated sheets, they were submerged into silica sol for 30 min. Then the sheets were dried in an oven at 100 °C for 2 h. This process was repeated 4–5 times. After that, the sheets were submerged into the LiCl solution for 12 h and then dried in an oven at 100 °C for 6 h [89]. Aluminum sections were dip-coated by preparing a suspension of SAPO 34 AQSOA-Z02 [90,93] or TiAPSO [94] solid desiccant. Particles of the solid desiccant were incorporated in a liquid solution, which had been in an ultrasonic bath for 30 min. The aluminum sections were immersed in the solution and later removed and dried at 250 °C [93,94]. The procedure allows us to obtain a solid desiccant coating layer between 0.2 [mm] to 0.8 [mm] thickness depending on the viscosity of the binder and solid desiccant suspension. For the use of zeolite SAPO-34 and silane-based binder [96], a two-step dip process was followed, in which the first coating consistent only in a binder and the second one in a solution of binder and solid desiccant. The pretreated aluminum sections were immersed in a binder-suspension for 1 [min] and cured during 30 [min] [96] or 20 [min] [95] at 80 °C. After this base layer binder coating, the aluminum sections were immersed in a binder and desiccant suspension for 1 [min] and cured for 2 h [96] [92] or 48 h [95] at 80 °C. The solid desiccant layer obtained had a thickness of 0.1 [mm]. Fig. 8 shows a flowchart of the two-step coating process. A procedure with higher curing temperatures was used to produce a heat exchanger with an RD-type silica gel coating [92]. In this case, the solid desiccant particles had first to be ground down to 0.07 [mm] particles, and HydroxyEthyl Cellulose (HEC) was used as the binder material. Finally, the heat exchanger was cured for 12 h at 120 °C.

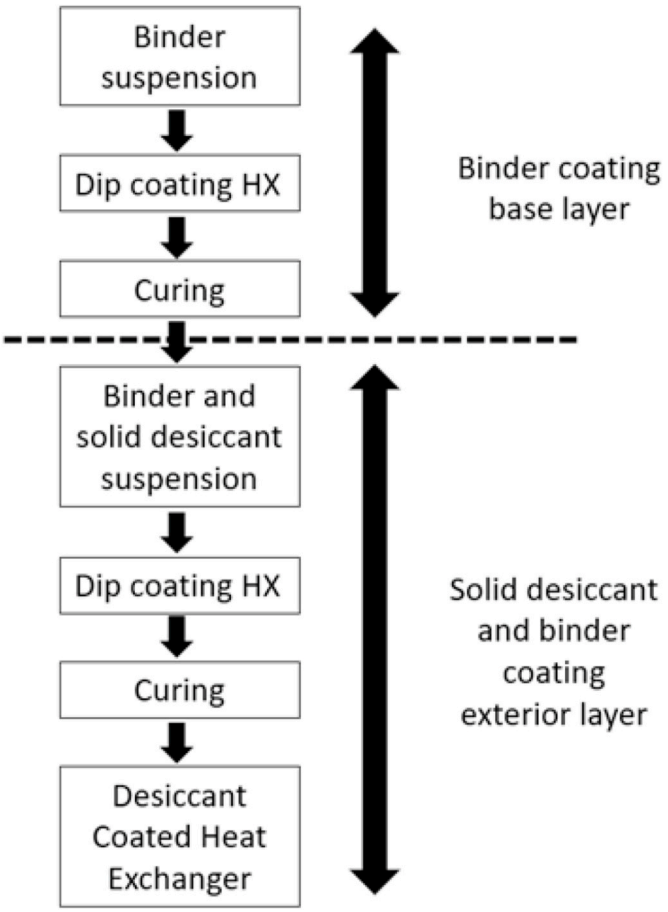


**Fig. 8.** Two-step dip-coating process, reproduction [96].

*5.2.1.2. Electrostatic spraying.* Another method to produce solid desiccant-coated surfaces is the use of electrostatic spraying [97], in which an Ion Exchange Resin (IER) is modified (MIER) by the impregnation method with lithium or magnesium. The impregnation was performed by immersing the IER into a 1 [mol/L] lithium or magnesium solution for 2 h and kept at 30 °C or 70 °C for lithium and magnesium. The MIER particles of adequate size were mechanically stirred and mixed with polymer powder coating. For the coating process, the mixture of MIER and polymer powder was loaded into the electrostatic device, and the coating procedure was performed at room temperature and 20 % relative humidity. The coated heat exchanger was curated at 130 °C for 15 min and finally cooled down at room temperature. This procedure produced a solid desiccant layer of 120 [μm]. If the sample is cured for a shorter time or at a lower temperature, the solid desiccant coating does not adhere adequately to the surfaces, and if cured during longer periods or at higher temperatures, the coating layer cracks.

*5.2.2. Direct synthesis of solid desiccant over the substrate*

A direct crystallization process can be used [91,98]to create zeolite layers. This process has been used to coat graphite foam with SAPO-34 zeolite [91]. The graphite foam underwent an oxidation process exposed to the air at 350 °C for 12 h to improve the surface for zeolite growth. The SAPO-34 zeolite deposition in the foam was produced by immersing the graphite foam samples in the solution of the zeolite at 200 °C for 72 h. After finishing the synthesis process, the foam samples were dried at 80 °C and finally calcinated at 500 °C for 12 h to remove impurities from the SAPO-34 zeolite. The direct synthesis was also used to produce metal surface coated on aluminum silicate and aluminum phosphor silicate zeolites [98]. The metal samples used were stainless steel, copper, and aluminum. To produce the samples coated on aluminum silicate zeolites (4A and Y), the zeolite precursors solution was maintained for 24 h at room temperature, and later the metal sections were immersed for 4 h at 95 °C. The metal sections were removed and dried at 80 °C. The immersion of the metal samples in the surface lasted 72 h and was kept at 200 °C, and later dried to produce samples coated on aluminum phosphor silicate zeolites. Table 5 resumes the reviewed solid desiccant coated methods. Aspects such as process required time, temperatures, and materials used are compared for each process.

## 6. Desiccant coated heat exchangers vs. Uncoated heat exchangers performance comparison

Airspeed in DCHEs influences the heat transfer, pressure drop, and the adsorption process in DCHEs. For this reason, for the following comparison, the properties have been compared to the closest possible range to that used on DCHE references, specifically, airspeed, in which the values commonly used in DCHE studies range between 0.5 and 2.5 [m/s] [3,69,99].

The coating of solid desiccant materials reduces the heat transfer coefficient of the heat exchanger. This reduction can reach between 15 % and 30 % for fin and tube and microchannel heat exchangers, respectively [63,69]. Additionally, the pressure drop in a coated exchanger tends to be higher than its uncoated pressure loss, reaching up to 55 %–60 % increases for fin and tube [63,69] and microchannel heat exchangers [69].

Heat transfer capacity is relevant for DCHE designs because it is necessary to transfer adsorption heat from the solid desiccant to the cold water to sustain the dehumidification process. Therefore, the heat transfer performance must be maximized to improve DCHE performance. Also, the pressure loss is relevant for DCHE operation because the high-pressure loss would increase the energy expended on air movement, thus offsetting the possible energy-saving potential of DCHEs. The airside heat transfer surface is another relevant parameter for DCHE because it represents the area on which the solid desiccant can be deployed in contact with the air. The higher the surface per volume, the higher the amount of solid desiccant surface that can be exposed to humid air.

The mass transfer performance of coated and uncoated heat exchangers has been compared [63,69]. Microchannel and fin and tube have been considered in these studies, and the effect of doubling fin depth also has been studied. Several scenarios of air velocity and water temperatures were evaluated. It was found that the mass transfer coefficient is larger in the dehumidification process than in the regeneration and that the average mass transfer coefficient of microchannel heat exchangers is 15 % higher than that of fin and tube heat exchangers, and the moisture removal rate per area of microchannel heat exchangers is 150 % higher than fin and tube heat exchangers [69]. Regarding the effect of fin depth, the longer case presented a 40 % higher moisture removal rate for a 100 % increase in fin depth. However, the mass transfer coefficient per unit area in the shorter fin heat exchanger is almost twice as large as in the longer fin depth case [63]. Regarding operational parameters that affect the moisture removal performance of the DCHE, it was found that by increasing the air velocity or the cycle time, the instant moisture removal rate is reduced [63], but it increases when increasing the hot water temperature [63]. Increasing cold water temperature reduces moisture removal per unit area in microchannel and fin and tube heat exchangers [69].

### 6.1. Heat transfer coefficient

Heat transfer between the air and the heat exchanger removes the adsorption heat from the air during the dehumidification process. It is important to DCHE performance because if air increases its temperature, the adsorption potential diminishes. Also, rejecting adsorption heat in the DCHE reduces the need for sensible auxiliary cooling before supplying dehumidified air into the building. Besides airside heat transfer, another aspect relevant to the total heat transfer of the heat exchanger is the heat transfer between tubes internal surface and water. However, this review focuses on airside heat exchanger designs that can be suitable for DCHE applications. Therefore heat transfer enhancement for the inner water tube is not covered.

Table 6 shows the airside heat transfer coefficient for both coated

**Table 5**
Characteristics of coating processes reviewed.

| Coating process | References | Process time | Substrate | Solid desiccant | Process temperatures | Binder | Coating thickness |
|---|---|---|---|---|---|---|---|
| Dip coating | [54, 89–95] | Solution immersion: 1–30 min (LiCl 12 h) Curing and drying: 30 min to 12 h | Aluminum | SAPO-34, FAPO-34, AQSOA-Z02, silica gel-LiCl, RD silica gel, TiAPSO | Curing: 80–120 C Drying: 100 C | Silane, clay-based binder, hydroxyethyl cellulose (HEC) | 0.1–0.8 [mm] |
| Electrostatic spraying | [97] | Impregnation drying: 24 h Drying: 15 min | Aluminum | LiCl impregnated IER | Drying: 60 C Solidification: 130 C | Polymer powder coating | 0.12 [mm] |
| Direct synthesis | [91,98] | Immersion: 4–72 h Drying: 12 h Calcination: 12 h (Graphite substrate) | Graphite foam, aluminum, stainless steel, copper | SAPO-34, 4A, Y, AlPO zeolites | Immersion: 95–200 C Drying: 80 C Calcination: 500 C | None | Tens of microns |

and uncoated heat exchangers. The coated heat exchanger has been coated with solid desiccant, transforming a heat exchanger into a DCHE. The uncoated heat exchanger presented is relevant because it shows the potential of heat exchanger designs not yet implemented as DCHE devices compared to the more conventional methods given in the coated heat exchangers.

For coated heat exchangers, fin and tube heat exchangers present the lowest value of the heat transfer coefficient. The minimum value of the heat transfer coefficient of the metal foam is higher than the maximum heat transfer coefficient shown by fin and tube heat exchangers. In microchannel heat exchangers, there is an overlap between the heat transfer coefficients range, but the microchannel design shows the higher minimum and maximum values.

In the case of uncoated heat exchangers, lattice heat exchangers show the widest range and highest maximum value of the heat transfer coefficient. Close to the maximum values of the heat transfer coefficient of the lattice heat exchanger are the metal foam and tube and wires heat exchangers. In all 3 cases (lattice, metal foam, and wires), a similar structure is present. These structures tend to generate high turbulence in the fluid, which causes a higher heat transfer coefficient.

### 6.2. Pressure loss

Table 7 shows that the fin and tube design produces lower values of pressure drop for the solid desiccant-coated heat exchangers. For the lower ranges, the difference in pressure drop is tenfold between the fin and tube and the microchannel and metal foam designs.

The maximum values also show large differences in pressure drop, in which the metal foam heat exchangers reach the highest values, despite considering a slightly higher air velocity than the other designs.

In the case of uncoated designs shown in Table 7, fin and tube heat exchangers present the lowest maximum pressure drop values. Maximum air velocity is higher in tube and wires, metal foam, and lattice heat exchangers than in fin and tube heat exchangers. However, based on the minimum and maximum air velocity pressure drop, it is possible to assume that their pressure drop would still be higher than that for fin and tube heat exchangers at a similar air velocity.

Fin and tube heat exchangers present two favorable properties for their use as DCHE compared to the alternative designs reviewed, which are their lower pressure loss and their possible range of surface area to volume. However, they present the lowest heat transfer coefficient range from the cases studied. For this reason, alternative designs with higher heat transfer coefficients such as tube and wires, metal foams, and lattice heat exchangers might provide similar or even improved performance with less desiccant-coated surface area. Nevertheless, the designs that showed improved heat transfer coefficient also showed higher pressure loss, so the tradeoff between those characteristics must be evaluated at system-level energy consumption.

**Table 6**
Heat transfer coefficient comparison for uncoated heat exchangers.

| Solid desiccant | Design | References | Airside heat transfer coefficient [W/m$^2$K] | Air velocity range [m/s] |
|---|---|---|---|---|
| Coated | Fin and tube | [3,69,99] | 30–110 (Nusselt 0.205–0.235 for Re 210–530) | 0.4–2.6 |
| | Microchannel | [69] | 80–190 | 0.5–2.6 |
| Uncoated | Metal foam | [34] | 140–350 | 0.5–2.9 |
| | Fin and tube | [64,69] | 50–110 (Nusselt 16–70 for Re 1700–7500) | 0.4–2.6 |
| | Tube and wires | [59] [a], [66] | 170 - 310 (Nusselt 35–80 for Re 300–2000) | 1.4–3.1 |
| | Teardrop tube | [58] | 140–210, (wet and dry condition) | 2.5–2.6 |
| | Metal foam | [66,71] | 110–300 (Nusselt 28–60 for Re 300–2000) | 1–3.1 |
| | Microchannel | [69] | 125–225 | 0.4–2.6 |
| | Lattice | [71,74] | 90–340 (Nusselt 31–68 for Re 150–1000) | 1–3.1 |

[a] Data from this reference has been converted from the original reference to the shown units.

**Table 7**
Pressure loss comparison for uncoated heat exchangers.

| Solid desiccant | Design | References | Pressure loss [Pa/m] | Air velocity range [m/s] |
|---|---|---|---|---|
| Coated | Fin and tube | [3] [a], [69] [a] | 34–955 | 0.4–2.6 |
| | Microchannel | [69] [a] | 389–2000 | 0.4–2.6 |
| Uncoated | Metal foam | [34] | 300–4900 | 1–3.4 |
| | Fin and tube | [69] [a] | 136–682 | 0.4–2.6 |
| | Tube and wires | [59] [a], [66] | 100–2100 | 0.5–3.1 |
| | Microchannel | [69] [a] | 278–1278 | 0.4–2.6 |
| | Metal foam | [71] [a], [66] | 100–8400 | 1–3.1 |
| | Lattice | [71] [a] | 800–6400 | 1–3.1 |

[a] Data from this reference has been converted from the original reference to the shown units.

It is essential to consider that advances in any of the fields analyzed (solid desiccant materials, substrate materials, design, or manufacturing process) will require an optimization process of the other fields and operational conditions to provide the highest possible performance. Nevertheless, to cross-compare the effect of different DCHE cases and determine the most promising future development requires evaluating total energy consumption for standardized air dehumidification temperature, humidity, and airflow. Such a comparison between a wide array of different solid desiccant materials, DCHE geometry, or operational conditions has not been published to the authors' best knowledge. Therefore, the definition of which development field could produce a more significant impact on DCHE performance remains to be studied.

Despite the mentioned limitation, more focused attempts at the comparison of the effect on the performance of geometry or solid desiccant materials can be found [30,50,69]. Regarding DCHE geometry comparison, 15 % improvement on mass transfer coefficient and 125 % increase in pressure drop for microchannel DCHE compared to traditional fin and tube heat exchangers using the same solid desiccant material (silica gel). However, the total energy consumption in each case is not shown [69]. Other studies compared significantly different geometries such as packed bed and coated metal foam for the same solid desiccant (RD silica gel) and found that the packed DCHE presented a moisture removal rate 2.5 times higher with a pressure loss 25 times higher than the coated case. No indication of the total energy consumption of both cases is shown, so it is not clear if the increase in moisture removal capacity offsets the increase in pressure drop [30]. On the other hand, comparing the same DCHE geometry with different coating materials has shown that aluminum fumarate over silica gel can improve dehumidification and regeneration capacities (8 % and 11 %, respectively) [50].

Additionally, for alternative designs of heat exchangers to use as DCHE, operational parameters such as air velocity and water temperatures should be independently studied. Relying on operational parameters optimized for fin and tube heat exchangers might not provide optimum performance to different heat exchangers designs working as DCHE.

## 7. Challenges and opportunities

### 7.1. Current and alternative heat exchangers

The state-of-the-art developments for DCHE have mainly

concentrated on the conventional design, i.e., flat fin and round tube heat exchangers. Even with simple designs, there are significant limitations due to the potential clogging of the desiccants since only low fin density configurations have been adopted. The development of advanced heat exchangers provides new opportunities through the use of promising alternative designs such as microchannels and novel materials such as metal foams. Fin and tube heat exchangers present certain characteristics that justify their use in DCHE devices, such as their high commercial availability, low-pressure drop, and relatively moderate to the high surface area to volume ratios. Nevertheless, they present a lower heat transfer coefficient than other heat exchanger designs. The lower heat transfer coefficient directly impacts the dehumidification performance of the DCHE. The heat transfer coefficient influences the capacity to reject adsorption heat to the cooling water, which sustains the adsorption process for longer periods than other solid desiccant dehumidification devices without internal cooling. By sustaining the adsorption process for longer periods, DCHE reaches higher levels of moisture saturation on the solid desiccant material than other solid desiccant dehumidification devices. For this reason, the thorough study and comparison of DCHE based on alternative heat exchangers designs might provide better configurations with improved performance. Since DCHE devices are part of a whole dehumidification system, future studies of alternative heat exchanger designs are needed to evaluate the energy performance of the complete system, including the fan energy consumption impacted by the pressure drop of the heat exchanger and the hot and cold water generation systems.

### 7.2. New design and geometrical optimization

New heat exchanger design in the DCHE differs from the conventional fin and tube design. Parametric studies would be required to determine their optimum operation conditions for dehumidification, potentially involving different air velocities, water temperatures, and cycle time compared to those currently used in fin and tube heat exchangers.

### 7.3. Novel materials as substrate

The use of heat exchangers based on metal foams or lattice frames is a promising development area due to their high heat transfer coefficients and surface areas. However, there are challenges, such as the thermal contact resistance between metal foams and the tubes. The replacement of tubes by heat sinks, in which the thermal fluid circulates under a flat plate touch either the metal foam or lattice frame, might reduce the thermal contact resistance between the heat exchanger elements. One interesting finding of metal foams and lattice heat exchangers is that the nonuniform porosity section provides improved performance. The specific arrangement of the different porosities section influences the thermal performance of the heat exchanger. The findings support the development of nonuniform porosity, nonsymmetrical heat exchangers, and the optimized arrangement of the porosity for the desired airflow direction and velocity.

### 7.4. Effective coating procedures

Since lattice heat exchangers have not yet been used for solid desiccant coating, it is not studied the effect that the superficial finishing of additively manufactured metallic parts might have over the adherence of the solid desiccant layer. In case the finishing of additively manufactured parts has a higher rugosity than common metallic surfaces, it might be possible to reduce the number of binder materials used for coating, increasing the mass transfer coefficient of the solid desiccant layer. A similar effect could be obtained in the case of using higher rugosity surfaces in fin and tube and microchannel heat exchangers.

### 7.5. Deployment challenges and opportunities

the DCHE has been considered for deployment in a range of configurations. The focus has often been mainly on the device itself, with limited attention paid to the system configuration. Integration with renewable and waste energy sources to provide heat for the regeneration process should be studied to ensure that the DCHE provides dehumidification with lower primary energy consumption than traditional VCSs. Another area is the means to provide sensible cooling. It could be achieved at the DCHE using low-temperature chilled water or auxiliary cooling devices such as direct expansion cooling coils and direct or indirect evaporative cooling devices. The system-level efficiencies of these scenarios need to be compared to reach the most energy-efficient solution.

### 7.6. Advanced solid desiccants

The continuing development of advanced solid desiccant materials can help improve the performance of DCHE by providing materials with high maximum water uptake and water adsorption isotherm curves and low regeneration temperatures. The development of materials with low regeneration temperatures and high maximum moisture uptake capacity is a crucial step for improving the efficiency of DCHE dehumidification systems because it enables the use of low-grade energy sources for regeneration.

## 8. Conclusions

A review of the current advances in both solid-desiccant coated heat exchangers and heat exchanger design has been presented. This review focused on the DCHE device itself, its design, materials, and manufacturing processes, as well as designs of heat exchangers that might be suitable for solid-desiccant coating purposes. Additionally, a section of the review described the view of the authors regarding relevant areas for future development in the field. Relevant takeaway points from the review are shown below:

- Despite that research on DCHE has been focused on fin and tube heat exchangers, some authors have evaluated the performance of alternative designs with promising results.
- Currently, there is research in the development of heat exchangers that could be adapted for solid desiccant cooling applications to improve the performance of the systems. Specific areas of further development worth mentioning are the use of metal foam and lattice heat exchangers.
- An imperfect thermal contact might significantly decrease the heat performance of the heat exchangers, which in the case of DCHE, is already reduced by the coating layer. For this reason, the use of manufacturing methods like brazing would be a better choice to produce higher-quality thermal contact and should be the preferred method of assembly.
- In an additively manufactured heat exchanger, the thermal contact issue is mitigated by the possibility of generating complex shapes that would require several separate parts if they are built using traditional manufacturing methods.
- The binders required for securing the mechanical joining between the solid desiccant layer and the heat exchanger substrate produce a reduction of the mass transfer properties of the solid desiccant. Still, in some cases, they increase the heat transfer coefficient of the solid desiccant layer.
- Of those three coating methods reviewed, the direct synthesis method does not require the use of binder materials. However, it involves the possibility of submerging the heat exchanger in the precursor solution at the required temperature for extended periods. In contrast, dip coating makes use of already synthesized solid

desiccant material simplifying the coating process. However, care must be taken to generate a uniform coating layer.

- The heat transfer coefficient, pressure drop, and airside surface area have been compared between different designs. It shows that even though fin and tube heat exchangers present a lower pressure drop than other designs, their heat transfer coefficient, and airside surface area are lower than different designs such as microchannel, lattice, and metal foam. This comparison highlights possible future developments of solid desiccant-coated heat exchanger designs.

Working models of DCHE for experimental purposes have been successfully developed. However, there are challenges for transforming this technology into a commercially feasible alternative to vapor compression systems dehumidification. Further research in each of the heat exchanger device subjects covered in this review, along with system-level integration with waste and renewable energy sources and control systems, is required. And even more so, the advances in the heat exchanger device must be evaluated at the system level to ensure that they provide an effective and energy-efficient alternative to dehumidification by vapor compression systems.

## Declaration of competing interest

The authors declare that they have no known competing financial interests or personal relationships that could have appeared to influence the work reported in this paper.

## Acknowledgments

The authors would like to acknowledge the US Department of Energy, Building Technologies Office for the support for this research. This manuscript has been authored by UT-Battelle, LLC, under contract DE-AC05-00OR22725 with DOE. The US Government retains and the publisher, by accepting the article for publication, acknowledges that the US government retains a nonexclusive, paid-up, irrevocable, worldwide license to publish or reproduce the published form of this manuscript or allow others to do so, for the US government purposes. DOE will provide public access to these federally sponsored research results according to the DOE Public Access Plan (http://energy.gov/downloads/doe-public-access-plan).

## References

[1] American Society of Heating R and A-CE. ANSI/ASHRAE standard 55-2017 thermal environmental conditions for human occupancy. Atlanta, Georgia. 2017.
[2] Liu L, Bai Y, He Z, Deng L, Li X, Li J, et al. Numerical investigation of mass transfer characteristics for the desiccant-coated dehumidification wheel in a dehumidification process. Appl Therm Eng 2019 Sep 1;160:113944.
[3] Sun XY, Dai YJ, Ge TS, Zhao Y, Wang RZ. Experimental and comparison study on heat and moisture transfer characteristics of desiccant coated heat exchanger with variable structure sizes. Appl Therm Eng 2018 Jun 5;137:32–46.
[4] Zheng X, Ge TS, Wang RZ. Recent progress on desiccant materials for solid desiccant cooling systems. Energy 2014;74:280–94. Elsevier Ltd.
[5] Ge TS, Li Y, Wang RZ, Dai YJ. A review of the mathematical models for predicting rotary desiccant wheel. Renew Sustain Energy Rev 2008;12:1485–528.
[6] Vivekh P, Kumja M, Bui DT, Chua KJ. Recent developments in solid desiccant coated heat exchangers – a review. Appl Energy 2018;229:778–803. Elsevier Ltd.
[7] Thommes M, Kaneko K, Neimark Av, Olivier JP, Rodriguez-Reinoso F, Rouquerol J, et al. Physisorption of gases, with special reference to the evaluation of surface area and pore size distribution (IUPAC Technical Report). Pure Appl Chem 2015 Oct 1;87(9–10):1051–69.
[8] Zouaoui A, Zili-Ghedira L, ben Nasrallah S. Open solid desiccant cooling air systems: a review and comparative study. Renew Sustain Energy Rev 2016;54:889–917. Elsevier Ltd.
[9] Hastürk E, Ernst SJ, Janiak C. Recent advances in adsorption heat transformation focusing on the development of adsorbent materials. Curr Opin Chem Eng 2019;24:26–36. Elsevier Ltd.
[10] Hamed AM, Abd-Elrahman WR, El-Emam SH, Awad MM. Theoretical and experimental investigation on the transient coupled heat and mass transfer in a radial flow desiccant packed bed. Energy Convers Manag 2013 Jan;65:262–71.
[11] Bonello M, Micallef D, Borg SP. Flat bed desiccant dehumidification: a predictive model for desiccant transient characterisation using a species transport model within CFD. J Build Eng 2019 May 1;23:280–90.
[12] Hiremath CR, Kadoli R. Experimental studies on heat and mass transfer in a packed bed of burnt clay impregnated with CaCl2 liquid desiccant and exploring the use of gas side resistance model. Appl Therm Eng 2013;50(1):1299–310.
[13] Shamim JA, Hsu WL, Kitaoka K, Paul S, Daiguji H. Design and performance evaluation of a multilayer fixed-bed binder-free desiccant dehumidifier for hybrid air-conditioning systems: Part I – experimental. Int J Heat Mass Tran 2018 Jan 1;116:1361–9.
[14] Ramzy KA, Kadoli R, Ashok Babu TP. Improved utilization of desiccant material in packed bed dehumidifier using composite particles. Renew Energy 2011 Feb;36(2):732–42.
[15] Angrisani G, Roselli C, Sasso M. Effect of rotational speed on the performances of a desiccant wheel. Appl Energy 2013;104:268–75.
[16] Chung JD, Lee DY, Yoon SM. Optimization of desiccant wheel speed and area ratio of regeneration to dehumidification as a function of regeneration temperature. Sol Energy 2009 May;83(5):625–35.
[17] Tu R, Hwang Y. Efficient configurations for desiccant wheel cooling systems using different heat sources for regeneration. Int J Refrig 2018 Feb 1;86:14–27.
[18] Jani DB, Mishra M, Sahoo PK. Solid desiccant air conditioning - a state of the art review. Renew Sustain Energy Rev 2016;60:1451–69. Elsevier Ltd.
[19] Ge TS, Dai YJ, Wang RZ, Peng ZZ. Experimental comparison and analysis on silica gel and polymer coated fin-tube heat exchangers. Energy 2010;35(7):2893–900.
[20] Vivekh P, Islam MR, Chua KJ. Experimental performance evaluation of a composite superabsorbent polymer coated heat exchanger based air dehumidification system. Appl Energy 2020 Feb 15;260:114256.
[21] Ge TS, Dai YJ, Li Y, Wang RZ. Simulation investigation on solar powered desiccant coated heat exchanger cooling system. Appl Energy 2012 Dec;93:532–40.
[22] Hsu WL, Paul S, Shamim JA, Kitaoka K, Daiguji H. Design and performance evaluation of a multilayer fixed-bed binder-free desiccant dehumidifier for hybrid air-conditioning systems: Part II – theoretical analysis. Int J Heat Mass Tran 2018 Jan 1;116:1370–8.
[23] Ge TS, Qi D, Dai YJ, Wang RZ. Experimental testing on contaminant and moisture removal performance of silica gel desiccant wheel. Energy Build 2018 Oct 1;176:71–7.
[24] Tu YD, Wang RZ, Ge TS, Zheng X. Comfortable, high-efficiency heat pump with desiccant-coated, water-sorbing heat exchangers. Sci Rep 2017 Jan 12;7:40437.
[25] Wang HH, Ge TS, Zhang XL, Zhao Y. Experimental investigation on solar powered self-cooled cooling system based on solid desiccant coated heat exchanger. Energy 2016;96:176–86.
[26] Ge TS, Cao W, Pan X, Dai YJ, Wang RZ. Experimental investigation on performance of desiccant coated heat exchanger and sensible heat exchanger operating in series. Int J Refrig 2017 Nov 1;83:88–98.
[27] Zhao Y, Dai YJ, Ge TS, Wang HH, Wang RZ. A high performance desiccant dehumidification unit using solid desiccant coated heat exchanger with heat recovery. Energy Build 2016 Jan;116:583–92.
[28] Vivekh P, Bui DT, Islam MR, Zaw K, Chua KJ. Experimental performance evaluation of desiccant coated heat exchangers from a combined first and second law of thermodynamics perspective. Energy Convers Manag 2020 Mar 1;207:112518.
[29] Chai S, Sun X, Zhao Y, Dai Y. Experimental investigation on a fresh air dehumidification system using heat pump with desiccant coated heat exchanger. Energy 2019 Mar 15;171:306–14.
[30] Mohammed RH, Mesalhy O, Elsayed ML, Huo R, Su M, Chow LC. Performance of desiccant heat exchangers with aluminum foam coated or packed with silica gel. Appl Therm Eng 2020 Feb 5;166:114626.
[31] Xu F, Bian ZF, Ge TS, Dai YJ, Wang CH, Kawi S. Analysis on solar energy powered cooling system based on desiccant coated heat exchanger using metal-organic framework. Energy 2019 Jun 15;177:211–21.
[32] Nawaz K, Schmidt SJ, Jacobi AM. Effect of catalyst and substrate on the moisture diffusivity of silica-aerogel-coated metal foams. Int J Heat Mass Tran 2014;73:634–44.
[33] Wu XN, Ge TS, Dai YJ, Wang RZ. Review on substrate of solid desiccant dehumidification system. Renew Sustain Energy Rev 2018;82:3236–49. Elsevier Ltd.
[34] Nawaz K, Bock J, Jacobi AM. Thermal-hydraulic performance of metal foam heat exchangers under dry operating conditions. Appl Therm Eng 2017;119:222–32.
[35] Jamzad P, Kenna J, Bahrami M. Development of novel plate heat exchanger using natural graphite sheet. Int J Heat Mass Tran 2019;131:1205–10.
[36] Palomba V, Vasta S, Giacoppo G, Calabrese L, Gullì G, la Rosa D, et al. Design of an innovative graphite exchanger for adsorption heat pumps and chillers. Energy Procedia 2015:1030–40.
[37] Fong KF, Lee CK. Impact of adsorbent characteristics on performance of solid desiccant wheel. Energy 2018 Feb 1;144:1003–12.
[38] Kubota M, Hanaoka N, Matsuda H, Kodama A. Dehumidification behavior of cross-flow heat exchanger type adsorber coated with aluminophosphate zeolite for desiccant humidity control system. Appl Therm Eng 2017;122:618–25.
[39] Wei Benjamin Teo H, Chakraborty A, Fan W. Improved adsorption characteristics data for AQSOA types zeolites and water systems under static and dynamic conditions. Microporous Mesoporous Mater 2017 Jan;242:109–17.
[40] Ž Knez, Novak Z. Adsorption of water vapor on silica, alumina, and their mixed oxide aerogels. J Chem Eng Data 2001 Jul;46(4):858–60.
[41] Ignat M, Samoila P, Cojocaru C, Soreanu G, Cretescu I, Harabagiu V. Porous polymer/inorganic composite matrices as efficient desiccants for air dehumidification. Appl Surf Sci 2019 Sep 1;487:1189–97.
[42] Rajamani M, Maliyekkal SM. Chitosan reinforced boehmite nanocomposite desiccant: a promising alternative to silica gel. Carbohydr Polym 2018 Aug 15;194:245–51.

[43] Bareschino P, Diglio G, Pepe F, Angrisani G, Roselli C, Sasso M. Numerical study of a MIL101 metal organic framework based desiccant cooling system for air conditioning applications. Appl Therm Eng 2017 Jun;124:641–51.
[44] Yan J, Yu Y, Ma C, Xiao J, Xia Q, Li Y, et al. Adsorption isotherms and kinetics of water vapor on novel adsorbents MIL-101(Cr)@GO with super-high capacity. Appl Therm Eng 2015 Jun 2;84:118–25.
[45] Vivekh P, Bui DT, Wong Y, Kumja M, Chua KJ. Performance evaluation of PVA-LiCl coated heat exchangers for next-generation of energy-efficient dehumidification. Appl Energy 2019 Mar 1;237:733–50.
[46] Feng X, Qin M, Cui S, Rode C. Metal-organic framework MIL-100(Fe) as a novel moisture buffer material for energy-efficient indoor humidity control. Build Environ 2018 Nov 1;145:234–42.
[47] Cui S, Marandi A, Lebourleux G, Thimon M, Bourdon M, Chen C, et al. Heat properties of a hydrophilic carboxylate-based MOF for water adsorption applications. Appl Therm Eng 2019 Jan;95:303–12.
[48] Solovyeva Mv, Gordeeva LG, Krieger TA, Aristov YI. MOF-801 as a promising material for adsorption cooling: equilibrium and dynamics of water adsorption. Energy Convers Manag 2018 Oct 15;174:356–63.
[49] Towsif Abtab SM, Alezi D, Bhatt PM, Shkurenko A, Belmabkhout Y, Aggarwal H, et al. Reticular Chemistry in action: a hydrolytically stable MOF capturing twice its weight in adsorbed water. Inside Chem 2018 Jan 11;4(1):94–105.
[50] Erkek TU, Gungor A, Fugmann H, Morgenstern A, Bongs C. Performance evaluation of a desiccant coated heat exchanger with two different desiccant materials. Appl Therm Eng 2018 Oct 1;143:701–10.
[51] Li A, Thu K, Ismail A bin, Shahzad MW, Ng KC. Performance of adsorbent-embedded heat exchangers using binder-coating method. Int J Heat Mass Tran 2016 Jan 12;92:149–57.
[52] Karmakar A, Prabakaran V, Zhao D, Chua KJ. A review of metal-organic frameworks (MOFs) as energy-efficient desiccants for adsorption driven heat-transformation applications. Appl Energy 2020 Jul 1;269:115070.
[53] van Heyden H, Munz G, Schnabel L, Schmidt F, Mintova S, Bein T. Kinetics of water adsorption in microporous aluminophosphate layers for regenerative heat exchangers. Appl Therm Eng 2009 Jun;29(8–9):1514–22.
[54] Zheng X, Wang RZ, Ge TS, Hu LM. Performance study of SAPO-34 and FAPO-34 desiccants for desiccant coated heat exchanger systems. Energy 2015 Dec 15;93:88–94.
[55] Kummer H, Jeremias F, Warlo A, Füldner G, Fröhlich D, Janiak C, et al. A functional full-scale heat exchanger coated with aluminum fumarate metal-organic framework for adsorption heat transformation. Ind Eng Chem Res 2017 Jul 26;56(29):8393–8.
[56] Chang K sen, Chen MT, Chung TW. Effects of the thickness and particle size of silica gel on the heat and mass transfer performance of a silica gel-coated bed for air-conditioning adsorption systems. Appl Therm Eng 2005 Oct;25(14–15):2330–40.
[57] Li Z, Michiyuki S, Takeshi F. Experimental study on heat and mass transfer characteristics for a desiccant-coated fin-tube heat exchanger. Int J Heat Mass Tran 2015 Jun 11;89:641–51.
[58] Huang Z, Ling J, Bacellar D, Hwang Y, Aute V, Radermacher R. Airside thermal and hydraulic characteristics of compact bare tube heat exchanger under dry and wet conditions. Int J Refrig 2020;110:295–307.
[59] Arie MA, Hymas DM, Singer F, Shooshtari AH, Ohadi M. An additively manufactured novel polymer composite heat exchanger for dry cooling applications. Int J Heat Mass Tran 2020 Oct;147:118889.
[60] Nawaz K, Abdelaziz O. Separate sensible and latent cooling system: a preliminary analysis of a novel approach [Internet]. Oak Ridge 2017 Aug. Available from: http://www.osti.gov/scitech/.
[61] Sun M, Hu C, Zha L, Xie Z, Yang L, Tang D, et al. Pore-scale simulation of forced convection heat transfer under turbulent conditions in open-cell metal foam. Chem Eng J 2020 Jun 1;389:154427.
[62] Ho JY, Leong KC, Wong TN. Additively-manufactured metallic porous lattice heat exchangers for air-side heat transfer enhancement. Int J Heat Mass Tran 2020 Dec;150:119262.
[63] Sun XY, Dai YJ, Ge TS, Zhao Y, Wang RZ. Comparison of performance characteristics of desiccant coated air-water heat exchanger with conventional air-water heat exchanger – experimental and analytical investigation. Energy 2017 Oct 15;137:399–411.
[64] Unger S, Beyer M, Gruber S, Willner R, Hampel U. Experimental study on the air-side thermal-flow performance of additively manufactured heat exchangers with novel fin designs. Int J Therm Sci 2019 Sep;146:106074.
[65] Saleh MM, Al-Dadah R, Mahmoud S, Elsayed E, El-Samni O. Wire fin heat exchanger using aluminium fumarate for adsorption heat pumps. Appl Therm Eng 2020 Sep;164:114426.
[66] Kurian R, Balaji C, Venkateshan SP. Experimental investigation of near compact wire mesh heat exchangers. Appl Therm Eng 2016;108:1158–67.
[67] Fugmann H, Oltersdorf T, Schnabel L. Metal wire structures as heat transfer surface area enlargement-design study and potential analysis for air-to-water heat pumps. In: 12th international energy agency heat pump conference. Rotterdam, Netherlands; 2017.
[68] Fugmann H, Laurenz E, Schnabel L. Wire structure heat exchangers-new designs for efficient heat transfer. Energies 2017;10(9).
[69] Sun XY, Dai YJ, Ge TS, Zhao Y, Wang RZ. Heat and mass transfer comparisons of desiccant coated microchannel and fin-and-tube heat exchangers. Appl Therm Eng 2019 Jan;150:1159–67.
[70] Guarino S, Barbieri M, Pasqualino P, Bella G. Fabrication and characterization of an innovative heat exchanger with open cell aluminum foams. In: Energy procedia. Berlin, Germany; 2017. p. 227–32.
[71] Bai X, Zheng Z, Nakayama A. Heat transfer performance analysis on lattice core sandwich panel structures. Int J Heat Mass Tran 2019;143:118525.
[72] Chen KC, Wang CC. Performance improvement of high power liquid-cooled heat sink via non-uniform metal foam arrangement. Appl Therm Eng 2015;87:41–6.
[73] Bamorovat Abadi G, Kim DY, Yoon SY, Kim KC. Thermal performance of a 10-kW phase-change plate heat exchanger with metal foam filled channels. Appl Therm Eng 2016 Apr 25;99:790–801.
[74] Son KN, Weibel JA, Kumaresan V, Garimella S v. Design of multifunctional lattice-frame materials for compact heat exchangers. Int J Heat Mass Tran 2017;115:619–29.
[75] Lacaze J, Tierce S, Lafont MC, Thebault Y, Pébère N, Mankowski G, et al. Study of the microstructure resulting from brazed aluminium materials used in heat exchangers. Mater Sci Eng 2005 Dec 15;413–414:317–21.
[76] Pech-Canul MA, Guía-Tello JC, Pech-Canul MI, Aguilar JC, Gorocica-Díaz JA, Arana-Guillén R, et al. Electrochemical behavior of tube-fin assembly for an aluminum automotive condenser with improved corrosion resistance. Result Phys 2017;7:1760–77.
[77] Jeong J, Kim CN, Youn B, Kim YS. A study on the correlation between the thermal contact conductance and effective factors in fin-tube heat exchangers with 9.52 mm tube. Int J Heat Fluid Flow 2004 Dec;25(6):1006–14.
[78] Jeong J, Kim CN, Youn B. A study on the thermal contact conductance in fin-tube heat exchangers with 7 mm tube. Int J Heat Mass Tran 2006 Apr;49(7–8):1547–55.
[79] Scattina A. Numerical analysis of tube expansion process for heat exchangers production. Int J Mech Sci 2016 Nov 1;118:268–82.
[80] Tang D, Li D, Peng Y. Optimization to the tube-fin contact status of the tube expansion process. J Mater Process Technol 2011 Apr 1;211(4):573–7.
[81] Kim CN, Jeong J, Youn B. Evaluation of thermal contact conductance using a new experimental-numerical method in fin-tube heat exchangers. Int J Refrig 2003 Dec;26(8):900–8.
[82] Kulshreshtha A, Dhakad SK. Preparation of metal foam by different methods: a review. Mater Today Proceedings [Internet] 2020 Mar;26. 1784–90. Available from: https://linkinghub.elsevier.com/retrieve/pii/S2214785320311305.
[83] de Schampheleire S, de Jaeger P, Huisseune H, Ameel B, T'Joen C, de Kerpel K, et al. Thermal hydraulic performance of 10 PPI aluminium foam as alternative for louvered fins in an HVAC heat exchanger. Appl Therm Eng 2013;51(1–2):371–82.
[84] T'Joen C, de Jaeger P, Huisseune H, van Herzeele S, Vorst N, de Paepe M. Thermo-hydraulic study of a single row heat exchanger consisting of metal foam covered round tubes. Int J Heat Mass Tran 2010 Jul;53(15–16):3262–74.
[85] Nematollahi O, Abadi GB, Kim DY, Kim KC. Experimental study of the effect of brazed compact metal-foam evaporator in an organic Rankine cycle performance: toward a compact ORC. Energy Convers Manag 2018;173:37–45.
[86] Bamorovat Abadi G, Moon C, Kim KC. Experimental study on single-phase heat transfer and pressure drop of refrigerants in a plate heat exchanger with metal-foam-filled channels. Appl Therm Eng 2016 Jun 5;102:423–31.
[87] Hathaway BJ, Garde K, Mantell SC, Davidson JH. Design and characterization of an additive manufactured hydraulic oil cooler. Int J Heat Mass Tran 2018;117:188–200.
[88] Ho JY, Leong KC, Wong TN. Experimental and numerical investigation of forced convection heat transfer in porous lattice structures produced by selective laser melting. Int J Therm Sci 2019;137:276–87.
[89] Zheng X, Ge TS, Jiang Y, Wang RZ. Experimental study on silica gel-LiCl composite desiccants for desiccant coated heat exchanger. Int J Refrig 2015;51:24–32.
[90] Freni A, Frazzica A, Dawoud B, Chmielewski S, Calabrese L, Bonaccorsi L. Adsorbent coatings for heat pumping applications: verification of hydrothermal and mechanical stabilities. Appl Ther Eng 2013:1658–63.
[91] Bonaccorsi L, Bruzzaniti P, Calabrese L, Freni A, Proverbio E, Restuccia G. Synthesis of SAPO-34 on graphite foams for adsorber heat exchangers. Appl Therm Eng 2013;61:848–52.
[92] Oh SJ, Ng KC, Chun W, Chua KJE. Evaluation of a dehumidifier with adsorbent coated heat exchangers for tropical climate operations. Energy 2017 Oct 15;137:441–8.
[93] Kummer H, Füldner G, Henninger SK. Innovative water vapor permeable coatings suitable for the use in adsorption chillers and heat pumps. Heat powered cycles [Internet]. Netherlands: Alkmaar; 2012. Available from: https://www.researchgate.net/publication/260316676.
[94] Munz GM, Bongs C, Morgenstern A, Lehmann S, Kummer H, Henning HM, et al. First results of a coated heat exchanger for the use in dehumidification and cooling processes. Appl Therm Eng 2013 Nov 3;61(2):878–83.
[95] Calabrese L, Brancato V, Bonaccorsi L, Frazzica A, Caprì A, Freni A, et al. Development and characterization of silane-zeolite adsorbent coatings for adsorption heat pump applications. Appl Therm Eng 2017;116:364–71.
[96] Freni A, Bonaccorsi L, Calabrese L, Caprì A, Frazzica A, Sapienza A. SAPO-34 coated adsorbent heat exchanger for adsorption chillers. Appl Therm Eng 2015 May 5;82:1–7.
[97] Fang Y, Zuo S, Liang X, Cao Y, Gao X, Zhang Z. Preparation and performance of desiccant coating with modified ion exchange resin on finned tube heat exchanger. Appl Therm Eng 2016 Jan 25;93:36–42.
[98] Bonaccorsi L, Calabrese L, Freni A, Proverbio E, Restuccia G. Zeolites direct synthesis on heat exchangers for adsorption heat pumps. Appl Ther Eng 2013:1590–5.
[99] Zhao Y, Dai YJ, Ge TS, Sun XY, Wang RZ. On heat and moisture transfer characteristics of a desiccant dehumidification unit using fin tube heat exchanger with silica gel coating. Appl Therm Eng 2015 Dec 5;91:308–17.